ABSTRACT

Title of Thesis: **STRUCTURAL AND FUNCTIONAL STUDIES OF CYCLIC K48-LINKED DIUBIQUITIN**

Adithya Sundar, Master of Science, 2016

Thesis Directed By: Professor David Fushman
Department of Chemistry and Biochemistry

K48-linked di-ubiquitin exists in a dynamic equilibrium between open and closed states. The structure of K48-Ub_2 in the closed conformation features a hydrophobic interface formed between the two Ub domains. The same hydrophobic residues at the interface are involved in binding to ubiquitin-associated (UBA) domains. Cyclization of K48-Ub_2 should limit the range of conformations available for such interactions. Interestingly, cyclic K48-linked Ub_2 ($cycUb_2$) has been found *in vivo* and can be isolated *in vitro* to study its structure and dynamics.

In this study, a crystal structure of $cycUb_2$ was obtained, and the dynamics of $cycUb_2$ were characterized by solution NMR. The crystal structure of $cycUb_2$, which is in agreement with solution NMR data, is closed with the hydrophobic patches of each Ub domain buried at the interface. Despite its structural constraints, $cycUb_2$ was still able to interact with UBA domains, albeit with lower affinity.

STRUCTURAL AND FUNCTIONAL STUDIES OF CYCLIC K48-LINKED DIUBIQUITIN

by

Adithya Sundar

Thesis submitted to the Faculty of the Graduate School of the
University of Maryland, College Park, in partial fulfillment
of the requirements for the degree of
Master of Science
2016

Advisory Committee:
Professor David Fushman, Chair
Professor Douglas Julin
Professor John Orban

Dedication

To Moose, for guiding me on my spiritual journey.

Acknowledgements

First and foremost I must express my gratitude towards my advisor Dr. David Fushman for his continuous support and guidance. I would also like to thank past and present committee members Dr. Douglas Julin, Dr. John Orban, and Dr. Paul Paukstelis for their insight on my projects.

I would like to thank Dr. Nicole LaRonde and Dr. Paul Paukstelis for their efforts in determining crystal structures of $cycUb_2$ and $cycUb_3$. Thank you to Dr. Carlos Castañeda for obtaining and analyzing experimental SANS data, and to Dr. Daoning Zhang for help with using the NMR spectrometers.

Thank you to Dr. Rajesh Singh for teaching me everything I know about biochemical and microbiological techniques in the lab.

Thank you to my fellow lab members: Alex, Andrew B., Andrew T., Apurva, Betsegaw, Christina, Donald, Dulith, Emma, Karina, Konstantin, Meredith, Ming-Yih, Tanuja, Urszula, Yaniv.

I would also like to thank my close friends and family for their love and support, which allowed me to persevere through difficult times.

Table of Contents

List of Tables

List of Figures

List of Abbreviations

ATP	adenosine triphosphate
CSP	chemical shift perturbation
$cycUb_2$	cyclic K48-linked Ub_2
$cycUb_3$	cyclic K48-linked Ub_3
DNA	deoxyribonucleic acid
DUB	deubiquitinases
E. coli	Escherichia coli
ESI-MS	electrospray ionization mass spectrometry
HECT	homologous to the E6-AP carboxyl terminus
hHR23a	human homolog of Rad23a
HMQC	heteronuclear multiple-quantum correlation
HSQC	heteronuclear single-quantum correlation
HyTEMPO	4-hydroxy-2,2,6,6-tetramethylpiperidin-1-oxyl
IPTG	isopropyl β-D-1-thiogalactopyranoside
isoT	isopeptidase-T
K48-Ub_2	(acyclic) K48-linked Ub_2
K_d	dissociation constant
NEDD8	neural precursor cell expressed developmentally down-regulated protein 8
NOE	nuclear Overhauser effect
NMR	nuclear magnetic resonance

polyUb	polyubiquitin
RDC	residual dipolar coupling
RING	really interesting new gene
RMSD	root-mean-square deviation
Rpn10	regulatory particle non-ATPase 10
Rub1	related to ubiquitin protein 1
SANS	small-angle neutron scattering
SDS	sodium dodecyl sulfate
SDS-PAGE	SDS polyacrylamide gel electrophoresis
SOFAST	band-selective optimized flip angle short transient
TCEP	tris(2-carboxyethyl)phosphine
Ub	ubiquitin
UBA	ubiquitin-associated
UBC	ubiquitin-conjugating
UBL	ubiquitin-like
Ubp6	ubiquitin-specific protease 6
UIM	ubiquitin-interacting motif
USP	ubiquitin-specific protease
UQ1	ubiquilin-1

Chapter 1: Introduction

1.1 Ubiquitin

Ubiquitin is a highly conserved small protein, 76 amino acids in length, which modulates various cellular events including proteolysis, DNA repair, and regulation of the cell cycle[1]. Substrates can be post-translationally modified by ubiquitin in a process known as ubiquitination via the formation of an isopeptide bond between the C-terminus of ubiquitin and the preferred lysine of the substrate. Ubiquitin has seven lysines and one N-terminal amine, all of which can be ubiquitinated to form polyubiquitin (polyUb) chains[2]. The modification of a substrate by the different polyUb chains results in interactions with various proteins that shuttle the substrate to different cellular processes. The position of the isopeptide linkage dictates which proteins interact with it and what cellular processes the substrate will be shuttled to. For example, the attachment of a K48-linked polyUb chain onto a substrate signals it for degradation by a multisubunit cellular protease known as the 26S proteasome[1, 3], whereas substrates attached to K63-linked polyUb chains are implicated in various cellular functions including DNA repair, ribosomal function, and endocytosis[1, 4].

1.2 Ubiquitination

Ubiquitination is carried out by a sequence of enzymatic reactions involving three enzymes: E1, E2, and E3. Ubiquitin is activated by E1 in an ATP-dependent mechanism, followed by the formation of an E1~Ub thioester intermediate on the active cysteine of E1. This thioester bond is then transferred to the catalytic cysteine of the conjugating enzyme E2 after which an E3 ligase coordinates the formation of an isopeptide bond between the lysine of a substrate and the C-terminus of ubiquitin[2]. It is important to note that the presence of a double glycine motif on the C-terminus of ubiquitin is required for activation by E1[5]. PolyUb chains are formed as a result of the aforementioned enzymatic sequence and exist either as "free" polyUb chains or attached to a substrate. Ubiquitination is reversible; deubiquitinases (DUBs) are responsible for the disassembly of polyUb chains.

1.2.1 E1-E2-E3 Cascade

In humans and in many other organisms, there is mainly one E1 responsible for the activation of ubiquitin, and the mechanism by which it works is well known. First, ubiquitin binds E1 where it is in proximity to a molecule of ATP. The C-terminal glycine of ubiquitin gets adenylated and is subsequently transferred to the conserved active cysteine residue of E1 to form a thioester bond. After the transfer of the ubiquitin-adenylate intermediate to the active cysteine of E1, another ubiquitin molecule binds at the initial binding site to get adenylated. At one time, an E1 enzyme carries

two molecules of ubiquitin; one bound to the adenylation site, and one covalently linked to the active cysteine[2, 6]. E2 enzymes recognize the fully loaded form of E1 with a higher affinity than E1 alone[2, 7]. E2 enzymes bind E1 through a conserved motif to catalyze the transthiolation reaction in which the ubiquitin~E1 thioester is transferred to the active cysteine of E2. While the mechanism by which transthiolation is achieved is still unclear, it is speculated that the thioester transfer from E1 to E2 may occur during the conformational change that happens in the formation of ubiquitin~E1 thioester[8].

All ubiquitins are activated mainly by a single E1[9], but are transferred to a variety of E2s. As of now, at least 35 different E2 enzymes have been found to exist in eukaryotes. All E2s share a highly conserved ubiquitin-conjugating (UBC) domain, roughly 150-200 amino acids in length[10]. The UBC domain functions to interact with E1 and E3 enzymes as well as to catalyze the transthiolation reaction using its catalytic cysteine residue. E2s vary in the presence of N- and/or C-terminal extensions and have been classified on this basis. Class I E2s consist of only the UBC domain, Class II and III E2s have N- and C-terminal extensions respectively, and Class IV E2s have both N- and C-terminal extensions[10]. Due to this variability, E2 enzymes interact with different cognate E3 ligases and ultimately help to ubiquitinate different substrates.

Similar to E2s, a class of E3 ligases, known as HECT E3s, accepts the ubiquitin onto its catalytic cysteine residue before the final transfer onto the

substrate protein[11]. A different class of E3s, the RING finger E3s, coordinate the E2~Ub thioester intermediate and the substrate to catalyze transfer of ubiquitin onto the substrate[12]. E3s are known to be substrate specific, usually having one or a few substrates with which they interact. Due to this specificity, there are on the order of ~1000 E3 ligases in the cell[13].

1.2.2 E2-25k

Almost all E2 enzymes work together with E3s to ultimately transfer an ubiquitin onto the substrate. The ubiquitin conjugating enzyme E2-25k is unique in that it generates free K48-linked polyubiquitin chains without the aid of an E3 ligase[14], so essentially ubiquitin acts as the substrate. E2-25k is a Class III E2 enzyme; it has the conserved UBC domain with a C-terminal ubiquitin-associating (UBA) domain. The UBA domain consists of a three-helix bundle, which binds ubiquitin via hydrophobic interactions. E2-25k is the only E2 which has a UBA domain[10], and it has been shown that the UBA domain is necessary for E2-25k to generate free polyubiquitin chains. Without the UBA domain, E2-25k can still function, but at a lower efficiency[15] and with less linkage specificity towards K48[16]. From this it can be assumed that the UBA domain helps to coordinate ubiquitin molecules to increase the catalytic activity of E2-25k and maintain the specificity of the linkage.

1.3 Ubiquitin-like proteins

Several proteins that are related to Ub based on sequence similarity have been classified as ubiquitin like (UBL) proteins. Of this group, the

mammalian protein NEDD8, and its yeast homolog Rub1, has the highest sequence identity to Ub (~55%). UBLs undergo a similar post-translational modification of substrates utilizing their own set of E1, E2, and E3 enzymes[17]. NEDD8 can interact with enzymes from the ubiquitin pathway, E1 and E2-25k, albeit with lower efficiency. NEDD8 is activated by ubiquitin E1 but cannot polymerize via E2-25k. However, it was shown that NEDD8 could be conjugated to the *distal* end of a K48-linked Ub_3 using E2-25k, forming the heterotetramer NEDD8-Ub_3[18]. In discussions of ubiquitin chains, the term *distal* refers to the last domain that uses its C-terminus in the isopeptide bond.

Recent studies have demonstrated that Rub1 forms Rub1-Ub heterodimers using ubiquitin E1 and E2-25k[19]. Like NEDD8, Rub1 alone was not able form homopolymers using E2-25k, and with Ub, Rub1 was only used as the distal domain of the heterodimer. It seems that Rub1 must be activated by ubiquitin E1 and transthioesterified onto E2-25k, forming the thioester intermediate E2-25k~Rub1. However, the reaction does not proceed unless Ub is present, in which case Rub1-Ub is produced. E2-25k is not able to recognize Rub1 as an acceptor domain in the reaction and therefore K48 of Rub1 is not able to attack the thioester to form Rub1-Rub1 chains. The differences between Rub1 and Ub that allow E2-25k to select specifically for Ub may provide information specifically about the step of the reaction at which the E2-25k~Ub thioester intermediate is attacked by K48 of the acceptor Ub.

1.4 K48-linked diubiquitin

1.4.1 Dynamic Equilibrium

Studies on the structure and dynamics of K48-linked dimer (K48-Ub_2) have shown that it exists in a dynamic equilibrium between closed and open conformations[20]. This dynamic equilibrium of K48-Ub_2 is modulated by pH; at low pH (4.5) it is predominantly open, while at neutral or high pH it is predominantly closed[21]. This is likely due to the presence of a histidine, H68, at the Ub-Ub interface. At low pH, the protonation of histidine (pK_a ~ 5.5) would introduce positive charges to both Ub domains, which would likely repel one another. Furthermore, the theoretical pI of Ub is 6.56, so there is also a bulk positive charge associated to each domain at lower pH.

The crystal structure 1AAR exemplifies the closed conformation of K48-Ub_2[22]. In this structure it is apparent that the two Ub domains form an interface wherein the hydrophobic patches of both Ub domains are buried (Figure 1-1). The canonical hydrophobic patch of Ub is primarily comprised of residues L8, I44, and V70[23]. These same residues that are involved in the Ub-Ub interface also play an important role in hydrophobic interactions with potential ligands of Ub or polyUb chains[24,25]. Therefore K48-Ub_2, while in the closed conformation, should not be able to bind to interacting proteins due to the sequestration of its hydrophobic patches. It seems that the dynamic nature of K48-linked polyUb chains in solution is what allows for it to interact with ligands under physiological conditions.

1.4.2 Cyclization of K48-Ub_2

The structure of K48-Ub_2, as shown in 1AAR, is highly compact and symmetrical. Given that there is an isopeptide bond between distal G76 and proximal K48, it is not surprising that distal K48 is in close proximity to proximal G76 (Figure 1-1). This indicates that it is possible to cyclize K48-Ub_2 through the formation of a second isopeptide bond between distal K48 and proximal G76. Indeed, cyclization of K48-linked polyUb chains was observed as a result of an *in vitro* ubiquitination reaction catalyzed by the E2 conjugating enzyme E2-25k[26]. Moreover, cyclic K48-Ub_2 ($cycUb_2$) was found to exist *in vivo*[27], demonstrating that cyclization of K48-linked chains is not simply just an artifact of *in vitro* ubiquitination reactions.

Given that $cycUb_2$ has been found *in vivo*, it is important to consider what role $cycUb_2$ may play in the cell. Due to its lack of free C-terminus, $cycUb_2$ cannot modify substrates or participate in polyUb chain elongation. Furthermore, the crystal structure of K48-Ub_2 in the closed conformation suggests that $cycUb_2$ is fixed in the closed conformation with the hydrophobic patch of each domain buried at the interface. This feature of its structure should render it incapable of binding ligands known to interact either with monoubiquitin or specifically known to bind to K48-linked chains. Surprisingly, individual apparent K_d values for domains binding to $cycUb_2$ and K48-Ub_2 were found to be similar[28]. This finding is unexpected based on our current understanding of how conformational dynamics of K48-linked polyUb chains play a necessary role in ligand binding.

A solution structure of cycUb$_2$ was determined based on NMR spectroscopy[29]. Interestingly, the ^{1}H-^{15}N HSQC spectrum of ^{15}N-labeled cycUb$_2$ produced a single set of peaks, due to its inherent symmetry. This is in contrast to acyclic K48-Ub$_2$ for which each Ub domain produces a slightly different set of peaks. The single set of peaks was assigned to the corresponding backbone amides of cycUb$_2$. Based on these assignments, and direct comparisons to spectra of monomeric Ub and K48-Ub$_2$, Hirano *et al.* came to the conclusion that K48-Ub$_2$ exists predominantly in the open conformation (~75%) at neutral pH. Their conclusion is inconsistent with all other approximations of K48-Ub$_2$ conformational equilibrium, determined by various methods[20, 21, 30], which reach the same conclusion that K48-Ub$_2$ is predominantly closed (~75%) at neutral pH.

Potentially, cycUb$_2$ could accumulate in the cell as a dead-end product if they are unrecognizable to DUBs. Cyclic K48-linked Ub$_3$ (cycUb$_3$), while resistant to many DUBs, disassembles into Ub monomers when incubated with bovine red blood cell extract[26]. It is not known exactly what component of bovine red blood cell extract possesses this ability to hydrolyze cycUb$_3$, nor is it known if this activity can be extended to cycUb$_2$ as well. Presumably, there must exist such a DUB that can digest cycUb$_2$, otherwise there would be an uncontrolled accumulation of cycUb$_2$, which would detract from the cellular Ub pool.

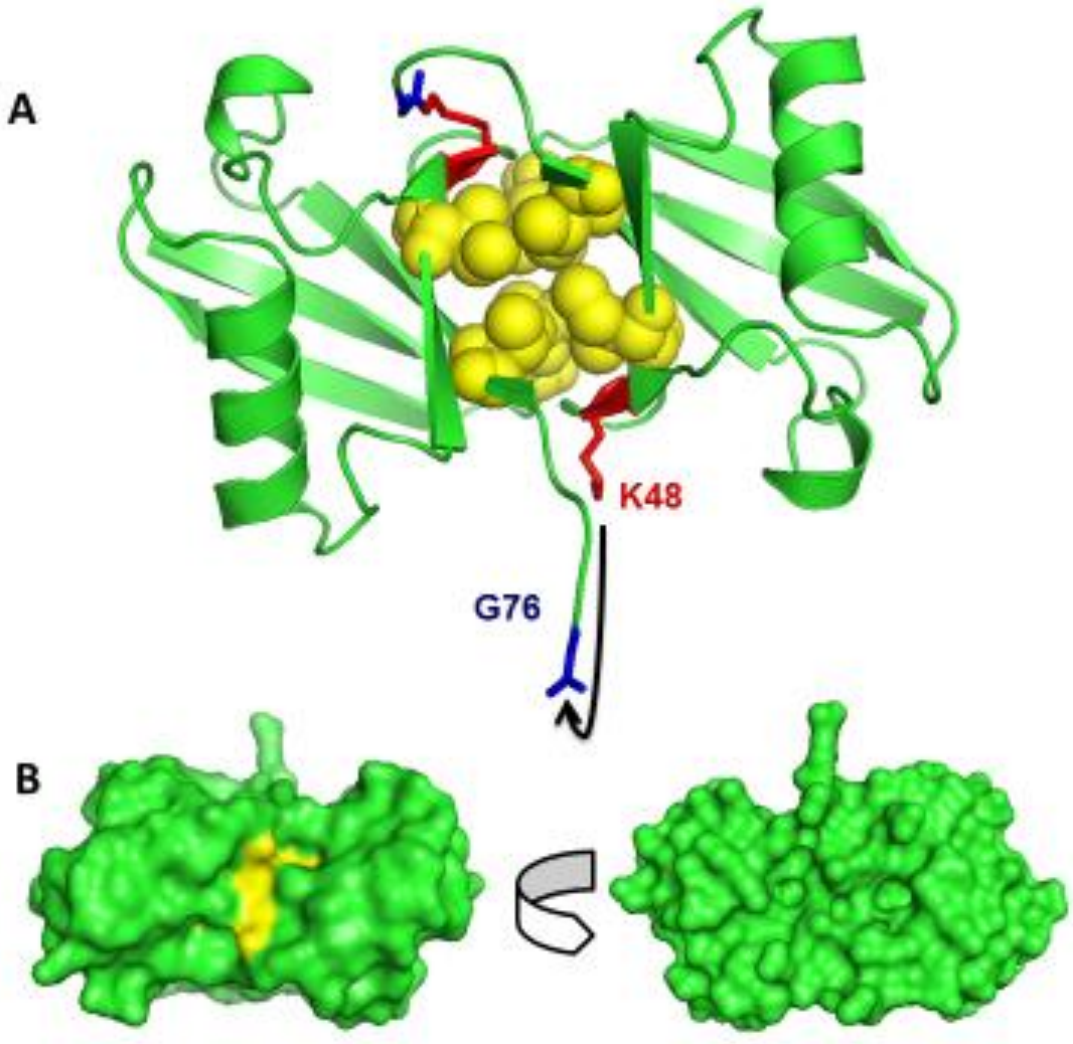

Figure 1-1: The proximity of distal K48 to proximal G76 suggests that cyclization of K48-Ub$_2$ can occur. A: Cartoon representation of K48-Ub$_2$ (PDB: 1AAR); hydrophobic patch comprised of L8, I44, and V70 shown as yellow spheres. B: The canonical hydrophobic patch of Ub is buried at the interface of K48-Ub$_2$. Surface representations of K48-Ub$_2$ (PDB: 1AAR); hydrophobic patch colored yellow.

1.5 Specific Aims

1.5.1 Cyclic K48-linked Ub_2

Utilization of the ubiquitin conjugating enzyme E2-25k in *in vitro* ubiquitination reactions allows for the formation of free K48-linked polyUb chains. Cyclized K48-linked polyUb chains, including $cycUb_2$ and $cycUb_3$, are formed as a result of these reactions. Not only does cyclization of K48-linked polyUb chains occur *in vitro*, quantitative analysis of endogenous Ub_2 from rat skeletal muscle revealed that $cycUb_2$ exists *in vivo*[27]. One could speculate that cyclic forms of free K48-linked polyUb chains of any length may occur *in vivo* as well; if $cycUb_2$ exists, then the same cellular machinery that created it may also produce higher order cyclic chains.

Current understanding of the nature of $cycUb_2$ is incomplete and requires further investigation. While the solution structure suggests that $cycUb_2$ is fixed in the closed conformation, $cycUb_2$ was still shown to have binding affinities towards interacting domains similar to those of K48-Ub_2[28]. A model of K48-Ub_2 in complex with a ubiquitin-associated (UBA) domain has been shown to involve an "opened" or "extended" conformation of K48-Ub_2[25]. Constrained by its second isopeptide bond, $cycUb_2$ likely cannot adopt such open conformations and therefore its mode of interaction should be different. The interaction between $cycUb_2$ and UBA domains should be closely examined to verify the binding affinities found and to determine the binding interface in order to create a model of the complex. The structure and

dynamics of $cycUb_2$ needs to be better understood to explain how such interactions could occur.

This thesis will address the following questions:

a. What is the structure of $cycUb_2$? Does $cycUb_2$ possess any dynamic properties—is it a fixed, rigid structure or can it "breathe"?

   The structure of $cycUb_2$ will be determined by X-ray crystallography. The dynamics of $cycUb_2$ in solution will be studied by NMR.

b. Is the hydrophobic patch in $cycUb_2$ accessible to ligands? If so, what is the binding mechanism?

   The affinity of $cycUb_2$ toward UBA domains will be determined and the mode of interaction will be characterized using NMR titrations.

c. Can $cycUb_2$ be disassembled by deubiquitinase activity?

   The activity of various deubiquitinases will be tested on $cycUb_2$.

1.5.2 E2-25k~Ub

The mechanism by which E2-25k works to produce K48-specific polyubiquitin chains remains unclear. Recently, we obtained the crystal structure of E2-25k in complex with a K48-linked ubiquitin dimer (unpublished data). Each unit cell contains one ubiquitin and one E2-25k molecule where ubiquitin is non-covalently bound to the UBA domain by its canonical hydrophobic patch. The crystal structure demonstrates that the

distance between K48 of the acceptor ubiquitin, which is bound to the UBA domain, and C92 of E2-25k is roughly 40Å (Figure 1-2).

In order for a nucleophilic attack to occur, this distance needs to be approximately 5Å or lower. This strongly suggests that a conformational change must occur to bring the lysine-48 of the acceptor ubiquitin in proximity to the thioester Ub~E2-25k. Finding the mechanism by which E2-25k is able to catalyze the formation of polyubiquitin chains would increase our current understanding of ubiquitination and may serve as a model for other related mechanisms.

It is possible that upon covalent modification of Ub onto its catalytic cysteine, E2-25k undergoes a conformational change, which brings the acceptor and donor Ub domains in proximity of one another. A model of E2-25k~Ub with Ub bound would serve to explore this possibility.

Specific Aims:

a. Create a stable E2-25k~Ub thioester intermediate mimic suitable for NMR experiments and crystal formation.
b. Study interaction between ubiquitin and E2-25k~Ub by NMR.

1.5.3 Rub1/Ub

Despite the high similarity between Rub1 and Ub, E2-25k is able to selectively polymerize Ub. This could be based on protein-protein interactions, or structural orientation of the molecules involved.

Specific Aims:

a. Mutational chimeric studies of Rub1 and Ub in combination with *in vitro* ubiquitination reactions will be done to reveal key residues that are required for ubiquitination.

b. NMR spectroscopy will be used to determine the surface of both Rub1 and Ub that is implicated in their interactions with E2-25k as well as to estimate the dissociation constant (K_d) of both interactions.

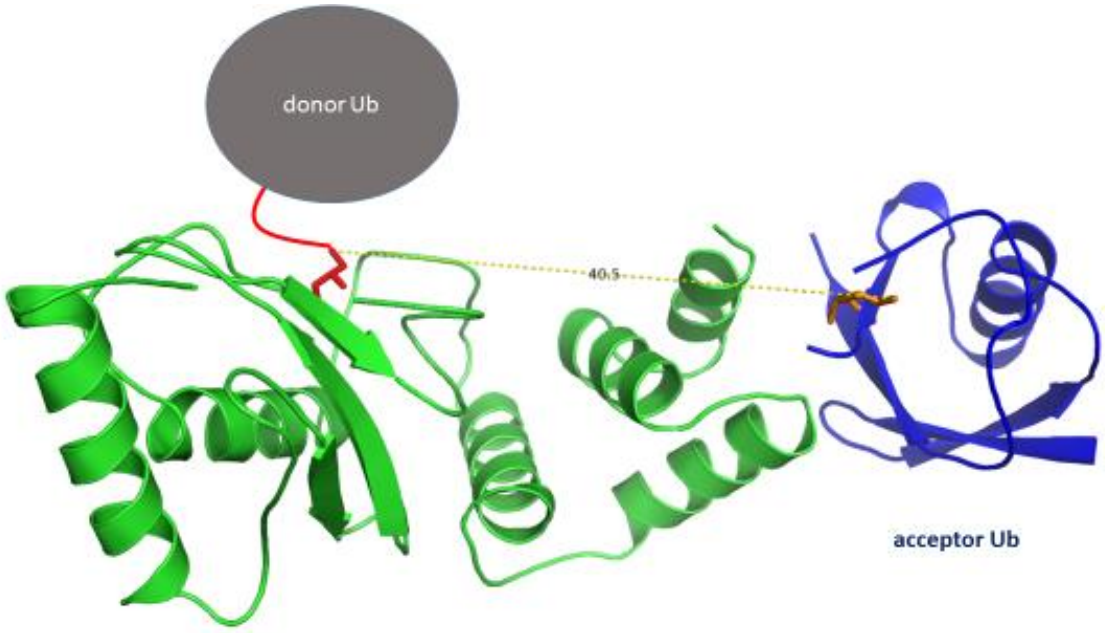

Figure 1-2: Crystal structure of E2-25k in complex with Ub. Cartoon representation of crystal structure of E2-25k (green) bound to Ub (blue). The catalytic cysteine, C92 (red), of E2-25k is shown to be approximately 40 Å away from K48 (orange) of the acceptor Ub. The donor Ub (gray) would be covalently attached to the catalytic cysteine via a thioester bond during the course of ubiquitination.

Chapter 2: Structural and Biochemical Studies of $CycUb_2$

2.1 Introduction

The ubiquitin conjugating enzyme E2-25k catalyzes the formation of unanchored K48-linked polyubiquitin (polyUb) chains *in vitro*. Some of these K48-linked polyUb chains become cyclized; a second isopeptide bond is formed between K48 of the distal Ub and G76 of the proximal Ub. It is likely that E2-25k, when charged with a polyUb, catalyzes the nucleophilic attack between the ε-amino group of distal K48 and the thioester at its active site, resulting in the formation of a cyclized product. In the closed conformation of K48-Ub_2, these residues are in close proximity to one another (Figure 1-1), allowing for cyclization to occur.

The dynamics and binding properties of K48-Ub_2 have been extensively studied and it seems advantageous for K48-Ub_2 to be able to open and close in order to interact with its binding partners. The same hydrophobic interactions responsible for stabilizing the closed conformation are used to bind its ligands. Upon cyclization, K48-Ub_2 may be fixed in the closed conformation, possibly hindering its capability to interact with its ligands. This possibility can be explored by characterizing the structure and dynamics of $cycUb_2$ in solution and by observing the interaction between $cycUb_2$ and ligands.

2.2 Formation and Isolation of cycUb$_2$

In order to characterize cycUb$_2$ *in vitro*, cycUb$_2$ had to be generated and isolated through a sequence of biochemical steps (Illustration 2-1). Wild type Ub was incubated in the presence of E1, E2-25k, ATP, and Mg^{+2} at 30˚C overnight to catalyze the formation of polyUb chains of varying lengths. Subsequently, these chains were treated with isoT (USP5) to cleave all acyclic chains into monoubiquitin, leaving the cyclic chains intact (Figure 2-1A). IsoT is a deubiquitinase that recognizes polyUb chains by its free C-terminus—a feature that is absent in cyclic chains. Therefore, from a mixture of cyclic and acyclic polyUb chains, isoT can specifically cleave acyclic chains while leaving cyclic polyUb chains intact.

Cyclic polyUb chains were then separated by cation exchange chromatography (Figure A-1) allowing for the isolation of cycUb$_2$ from the mixture. CycUb$_2$ was verified by ESI-MS (Figure 2-1B); the expected mass of cycUb$_2$ is 17093.6 Da; a mass of 17092.8 Da was observed. ^{15}N-labeled cycUb$_2$ was formed, purified, and also verified by mass spectrometry (Figure A-3); the construct was then used to study structural characteristics of cycUb$_2$ through NMR spectrometry.

From its ^{1}H-^{15}N 2D HMQC (SOFAST) spectrum, we can observe the shift of G76 from free to conjugated position (Figure 2-1C). No free G76 is observed, which further verifies that the construct is indeed cyclic and purified of any acyclic K48-Ub$_2$ or monoUb. Notably, only one set of peaks is observed due to the symmetric nature of cycUb$_2$. The two Ub domains are indistinguishable from one another by NMR, therefore the local chemical environment of each residue on either domain is exactly the same.

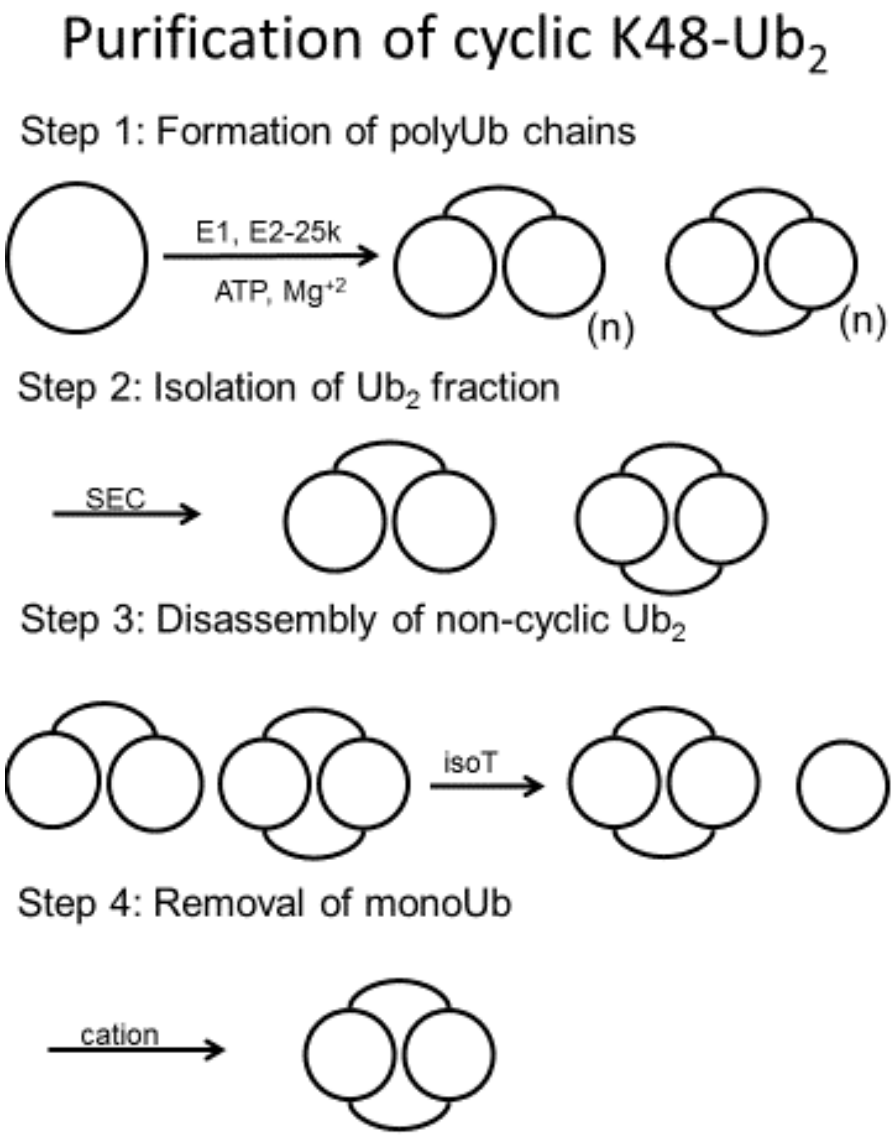

Illustration 2-1: Schematic overview of cycUb$_2$ purification. Step 1: E2-25k mediated *in vitro* ubiquitination reaction used to generate a mixture of cyclic and acyclic K48-linked chains. Step 2: Reaction mixture from Step 1 is passed through SEC column and fractions containing Ub$_2$ are preserved. Step 3: Ub$_2$ fractions are incubated with isoT to allow for the disassembly of acyclic K48-Ub$_2$ into monoUb. Step 4: Reaction mixture from Step 3 is purified by cation exchange chromatography, which allows for the separation of monoUb from cycUb$_2$.

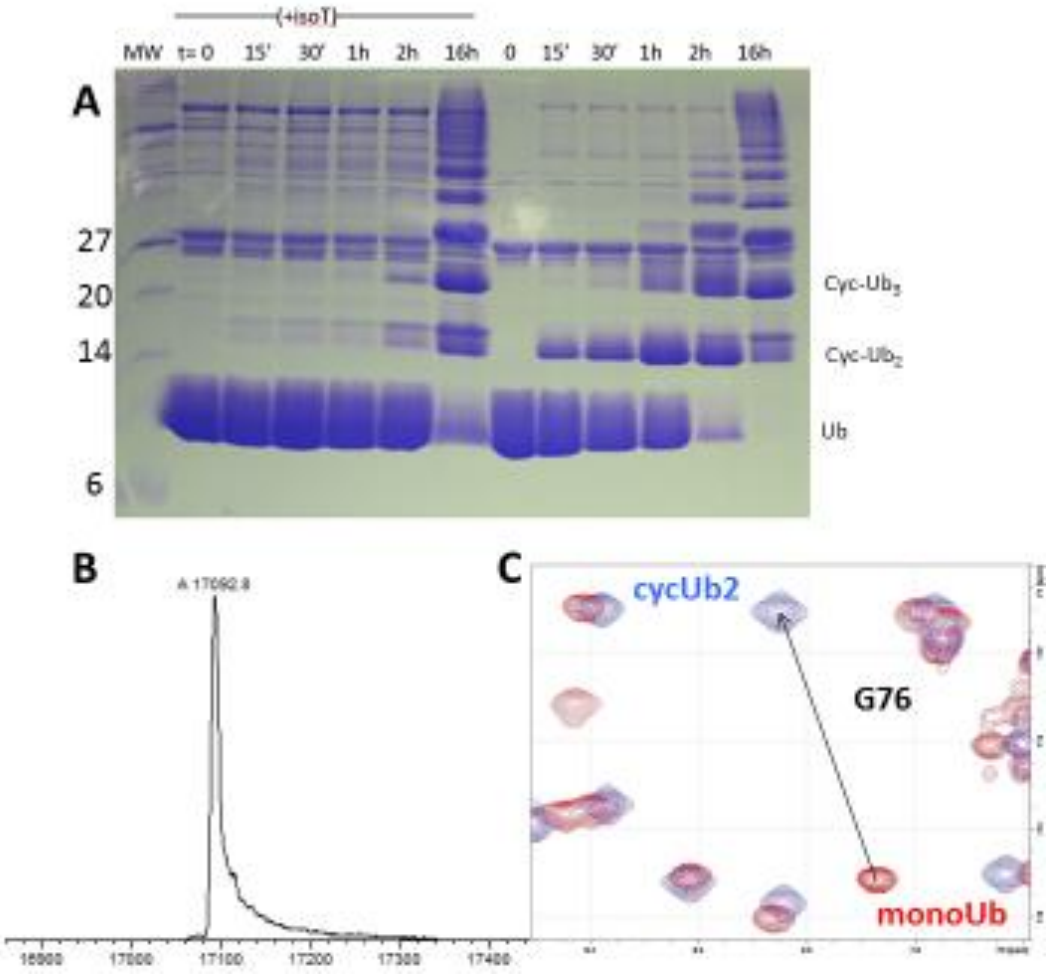

Figure 2-1: Formation of cyclic K48-linked polyUb chains. A: K48-linkage specific ubiquitination reaction catalyzed by E2-25k at various time points (t=0,15',30',1h,2h,16h), incubated with isoT at 37°C for 6h, and analyzed by 15% SDS-PAGE gel. B: ESI-MS spectrum of $cycUb_2$ (expected: 17093.6; observed: 17092.8). C: Overlay of ^{1}H-^{15}N HMQC spectra of $cycUb_2$ (blue) and monoUb (red).

2.3 Crystal Structure of cycUb$_2$

A solution containing pure cycUb$_2$ was screened against a variety of buffer conditions in hopes of achieving crystallization via hanging drop method. Several crystals with morphologies suitable for X-ray diffraction formed (Figure A-5), of which a select few were optimized under slightly varied pH levels and precipitant concentrations. Dr. Nicole LaRonde determined the structure with a resolution of 1.4Å (Table 2-1).

Based on this crystal structure, it seems that the majority of the hydrophobic patch of Ub is buried. Taking into consideration the canonical hydrophobic patch (L8, I44, and V70), in the crystal structure of cycUb$_2$, only 17% of its surface area is solvent accessible. In comparison, the same residues of monoUb (1D3Z) 53% of its surface area is solvent accessible.

Both isopeptide bonds between the two domains are observed (Figure 2-2). The crystal structure of cycUb$_2$ is very similar to the crystal structure of acyclic K48-Ub$_2$, 1AAR (RMSD = 0.34 Å). The difference between the two structures is primarily noticeable at the proximal C-terminus, which is untethered in acyclic K48-Ub$_2$. The high similarity between the two structures suggests that cycUb$_2$ can be used as a model of the closed conformation of K48-Ub$_2$.

Wavelength (Ã)	0.97741
Resolution range (Ã)	41.59 - 1.391 (1.441 - 1.391)
Space group	P1
Unit cell	24.972 30.342 45.503 70.97 74.25 84.58
Total reflections	90061
Unique reflections	23059 (2234)
Multiplicity	3.9 (3.8)
Completeness (%)	94.56 (91.44)
Mean I/sigma(I)	48.5 (15.7)
Wilson B-factor	11.64
R-merge	0.039 (0.094)
R-meas	0.046 (0.109)
CC1/2	0.995 (0.990)
CC*	0.998 (0.997)
Reflections used for R-free	1161 (145)
R-work	0.1231 (0.1089)
R-free	0.1640 (0.1822)
Number of non-hydrogen atoms	1485
macromolecules	1258
ligands	17
water	210
Protein residues	152
RMS(bonds)	0.009
RMS(angles)	1.28
Ramachandran favored (%)	99
Ramachandran allowed (%)	1
Ramachandran outliers (%)	0
Clashscore	3.06
Average B-factor	16.00
macromolecules	13.30
ligands	48.60
solvent	29.30

Table 2-1: Data collection and refinement statistics of cycUb$_2$ crystal. Statistics for the highest-resolution shell are shown in parentheses.

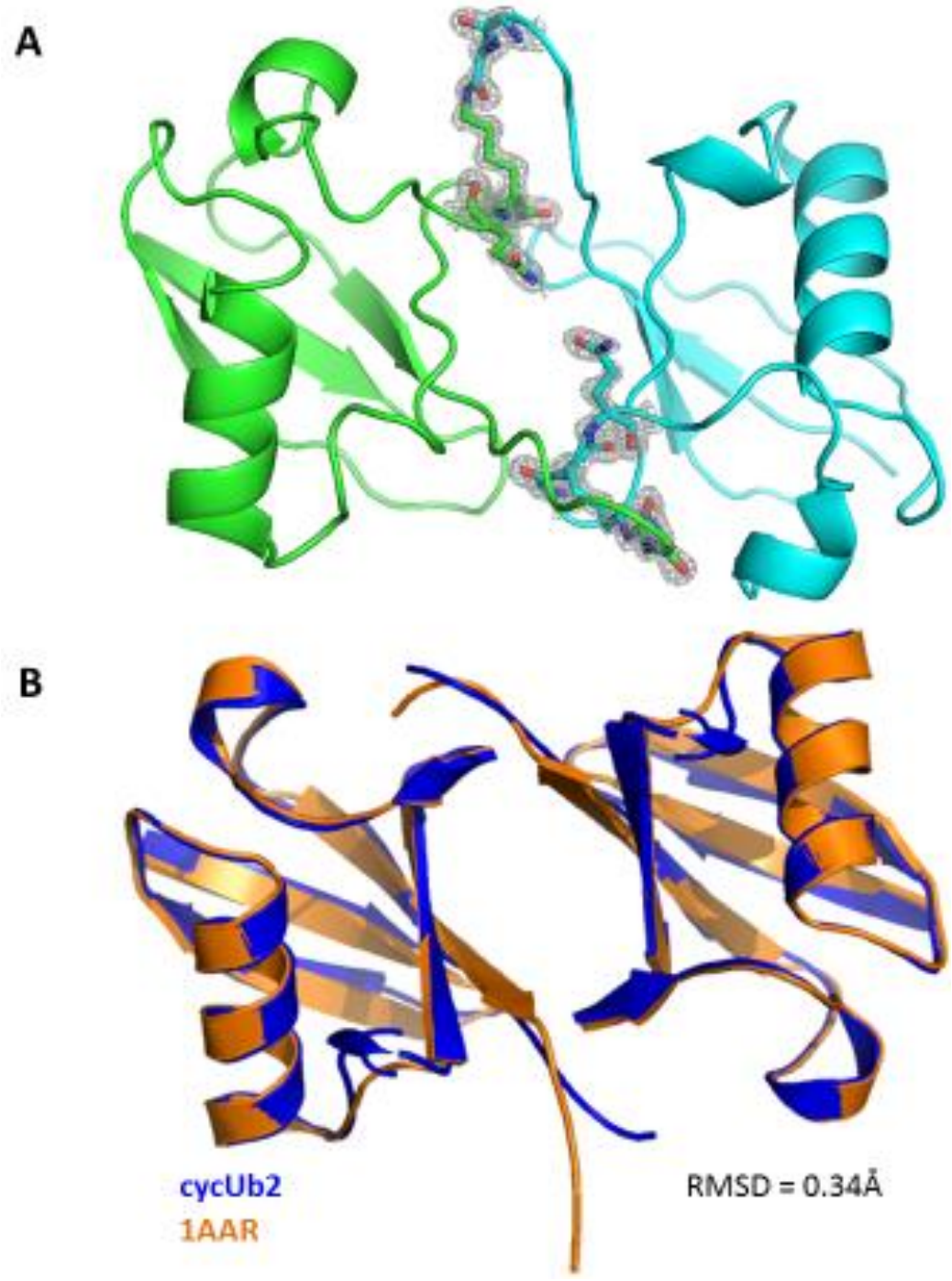

Figure 2-2: Crystal structure of cycUb$_2$. A: Cartoon representation of cycUb$_2$ with residues involved in isopeptide bonds shown as sticks surrounded by gray mesh indicative of electron density. B: Structure overlay of cycUb$_2$ (blue) with K48-Ub$_2$ (1AAR, orange).

2.3.1 Chemical shift perturbations mapped onto crystal structure

Despite having two Ub domains, a ^{1}H-^{15}N HSQC spectrum of isotopically labeled ^{15}N cycUb_2 has one set of chemical shifts corresponding to its backbone amide protons and nitrogens. Chemical shifts are very sensitive to the local chemical environment of the nuclei being observed. Changes to the local chemical environment of these nuclei can be observed by measuring chemical shift perturbations (CSPs). Comparing HSQC spectra of cycUb_2 with Ub yields significant CSPs; specifically, residues L8, A46, G47, V70, L73, G75, and G76 were most significantly perturbed (CSP > 0.3 ppm).

By mapping these CSPs onto the crystal structure of cycUb_2 we can see that the most highly perturbed residues are, as expected, found at the interface between the two Ub domains (Figure 2-3).

2.3.2 ^{1}H-^{15}N HMQC experiment

In solution, K48-Ub_2 exists in a dynamic equilibrium between open and closed conformations. The chemical shifts observed in a HSQC spectrum of K48-Ub_2 are a result of an average of all the conformations that K48-Ub_2 may exist in, assuming that the various conformations interconvert in the fast-exchange regime.

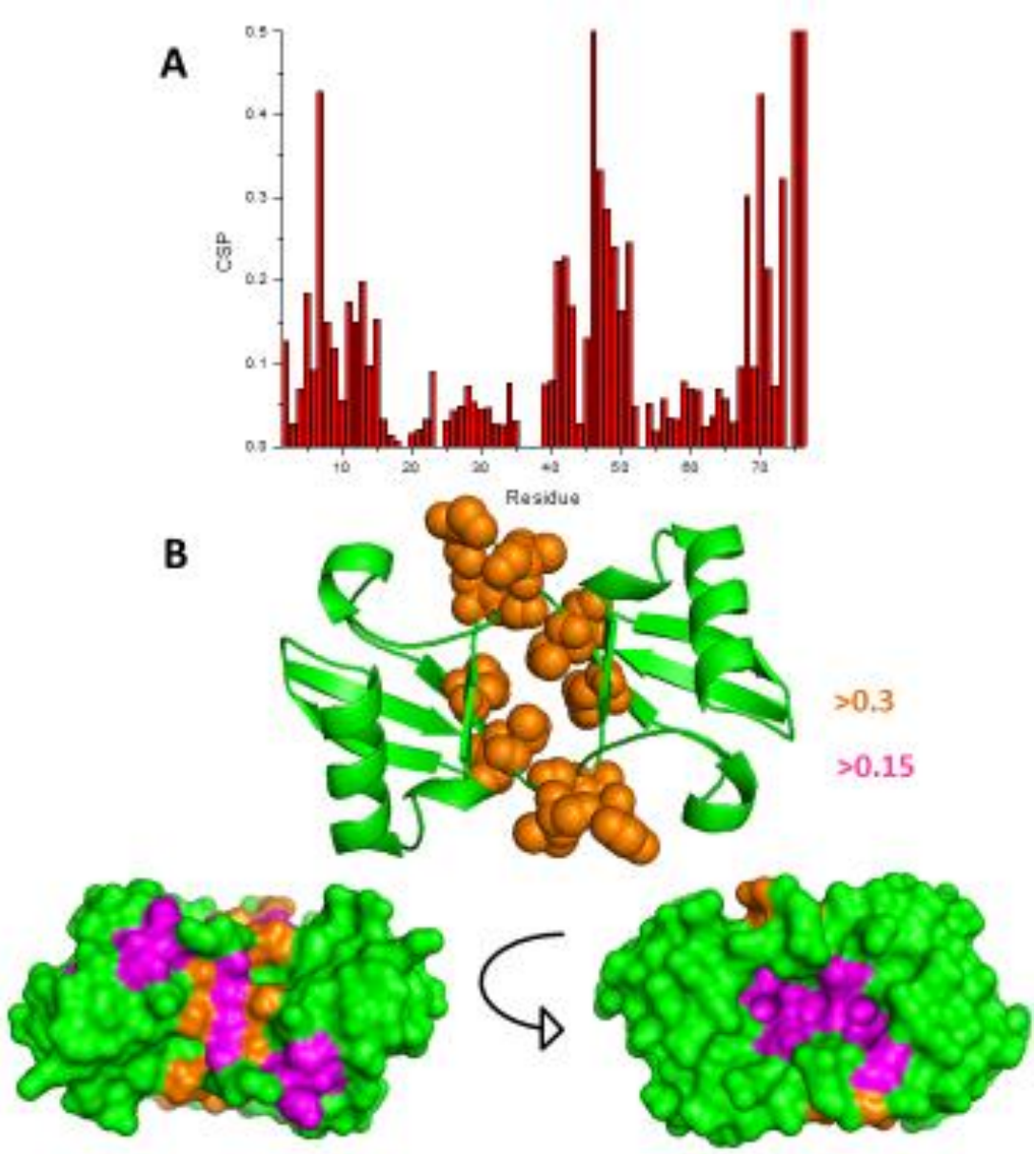

Figure 2-3: Chemical shift perturbations of cycUb$_2$ compared to monoUb mapped onto the crystal structure of cycUb$_2$. A: CSP plot of cycUb$_2$ compared to monoUb. B: Residues with significant CSPs (CSP>0.3, orange; CSP>0.15, magenta) mapped onto the surface of cycUb$_2$.

At neutral pH, K48-Ub_2 exists in predominantly closed conformations; at low pH, K48-Ub_2 exists in predominantly open conformations. This was evidenced by CSPs observed for K48-Ub_2 in comparison to Ub in buffers varying in pH[21]. At neutral pH, CSPs were observed for residues involved at the hydrophobic interface between the two Ub domains. These CSPs attenuated almost completely at low pH, indicating that the local chemical environment of these residues is similar to Ub while in the open conformation.

The HSQC spectrum of cycUb_2 is drastically different from either K48-Ub_2 or Ub in a residue-specific manner. Interestingly, the chemical shifts of the three species tend to fall on a path that is nearly linear; K48-Ub_2 generally lies between Ub and cycUb_2 (Figure 2-4). These residues with significant CSPs are found primarily at the hydrophobic interface. This seems to suggest that cycUb_2 is fixed in the closed conformation, whereas K48-Ub_2 is in a conformational exchange between open and closed conformations. Presumably, the presence of a second isopeptide bond must limit the range of conformations that cycUb_2 may take.

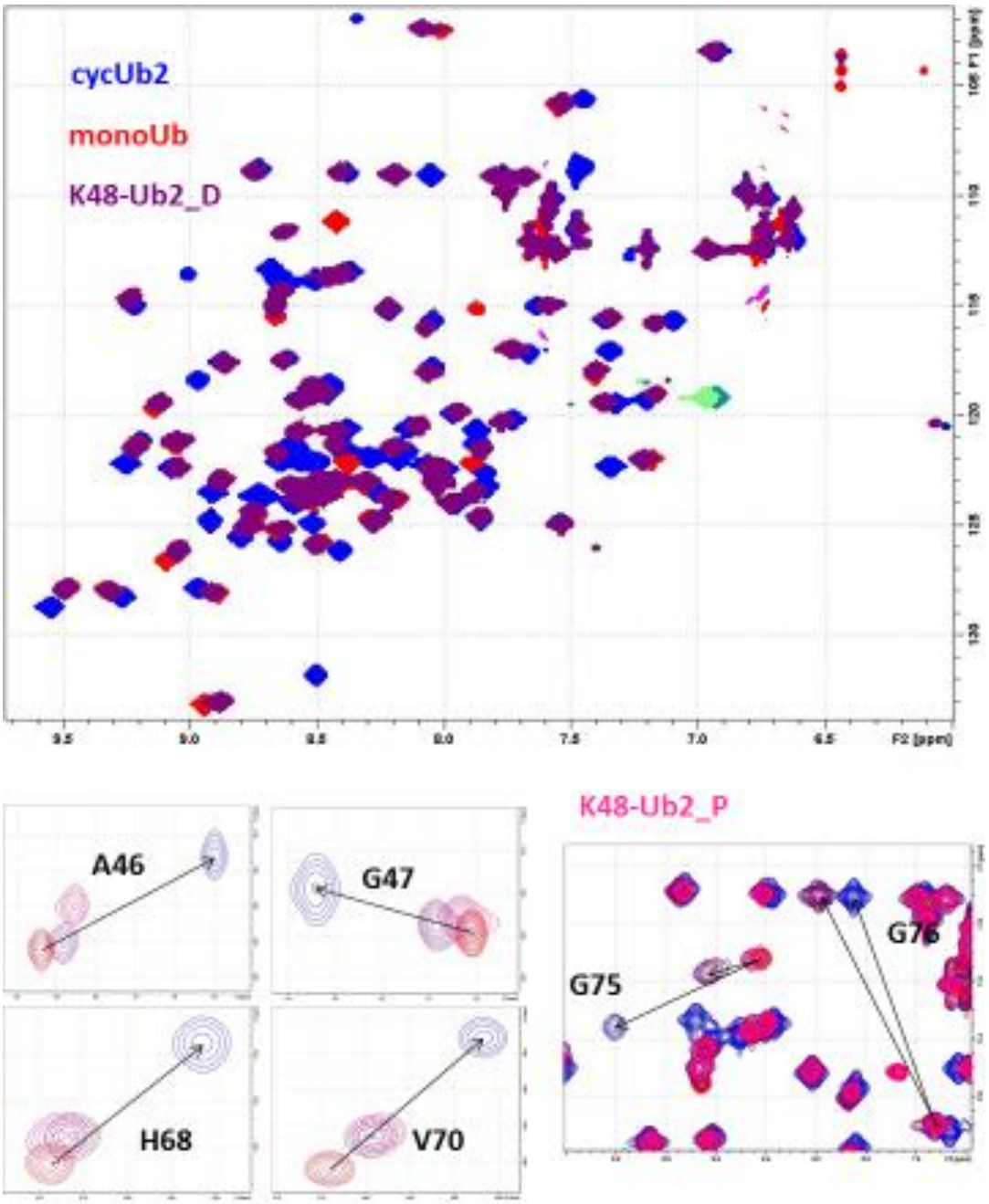

Figure 2-4: 1H-15N HMQC spectra of cycUb$_2$ in comparison with monoUb and K48-Ub$_2$. Overlay of cycUb$_2$ (blue), Ub (red), and K48-Ub$_2$ distal domain (purple). Proximal domain of K48-Ub$_2$ (pink) is included in zoomed-in spectra of residues A46, G47, H68, V70, G75, and G76.

2.4 Characterization of cycUb$_2$ in solution by NMR

2.4.1 Residual dipolar coupling measurements of cycUb$_2$

Residual dipolar coupling (RDC) experiments provide information about the relative orientation of protein domains. Dipolar couplings are measured by placing the isotopically labelled protein in a liquid-crystalline media such that anisotropy is achieved. Otherwise, if the media were isotropic, the dipolar couplings would average out to zero.

RDC data are in strong agreement with the NMR-derived solution structure of monoUb (PDB: 1D3Z) when considering one or both domains (Figure 2-5). When considering both domains, the orientation of the two Ubs with respect to one another is taken from the crystal structure of cycUb$_2$. Each Ub is replaced with 1D3Z to properly recreate the amide protons. From this information, RDC values are back-calculated and compared to experimental data ($r = 0.99$), suggesting that the relative orientation of Ub domains in the crystal structure of cycUb$_2$ is in agreement with what is observed in solution. Only taking the information given by the crystal structure and building amide protons according to standard peptide-plane geometries, we still get a good fit ($r = 0.93$) with the experimental RDC data.

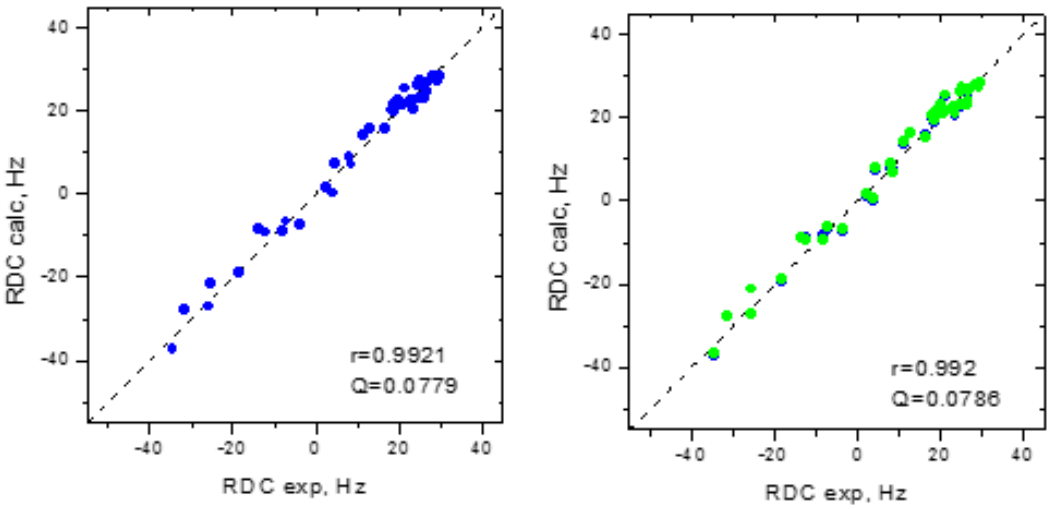

	S_x	S_y	S_z	α	β	γ	Asym	r	R
1D3z	27.6214	28.3081	-55.9295	294.596	66.480	127.255	0.012	0.99209	0.07791
1D3z (Xtal_D)	27.6197	28.3184	-55.9381	270.368	149.914	23.944	0.012	0.99209	0.07791
Xtal D	22.1475	30.4289	-52.5764	266.998	150.138	332.345	0.158	0.936	0.24075
Xtal P	22.2123	29.5432	-51.7555	273.445	150.148	32.498	0.142	0.934	0.229
Xtal_both	24.3899	28.4150	-52.8048	270.118	149.434	1.774	0.076	0.92905	0.24655
1D3z (Xtal_both)	27.6367	28.1652	-55.8019	269.9850	150.2310	-5.6320	0.009	0.99197	0.078585
Best orient of prox	27.6120	28.3120	-55.9239	270.375	149.903	22.136	0.013	0.99208	0.077964

Figure 2-5: Residual dipolar coupling data of cycUb$_2$. Agreement between experimental and back-calculated RDCs (PDB: 1D3Z) for individual Ub domains of cycUb$_2$, taking into consideration either one domain (blue) or both domains (green).

2.4.2 ^{15}N Relaxation experiments

T1, T2, and heteronuclear NOE (hetNOE) experiments give us information about the overall tumbling time and about local dynamics of the protein (Figure 2-6). Generally, hetNOE values correspond to the flexibility of the region; higher values (~0.8) indicate areas of low flexibility, lower values (<0.7) indicate areas of high flexibility. In $cycUb_2$, the flexible areas include the loop between β_1 and β_2 (residues 8-11) and the C-terminal tail (residues 71-76). The C-terminus of $cycUb_2$ has a loop-like character. Heteronuclear NOE values of the C-terminus of unconjugated Ub, either in the form of monoUb or a proximal domain of a polyUb, are much lower than what is observed for $cycUb_2$.

2.4.3 ROTDIF analysis

The diffusion tensor of $cycUb_2$, determined by analysis of relaxation data (ROTDIF), is in agreement with the predicted diffusion tensor (HYDRO) based on the crystal structure (Figure 2-7). Also the relative orientations of the two Ub domains agree well with the experimental relaxation data.

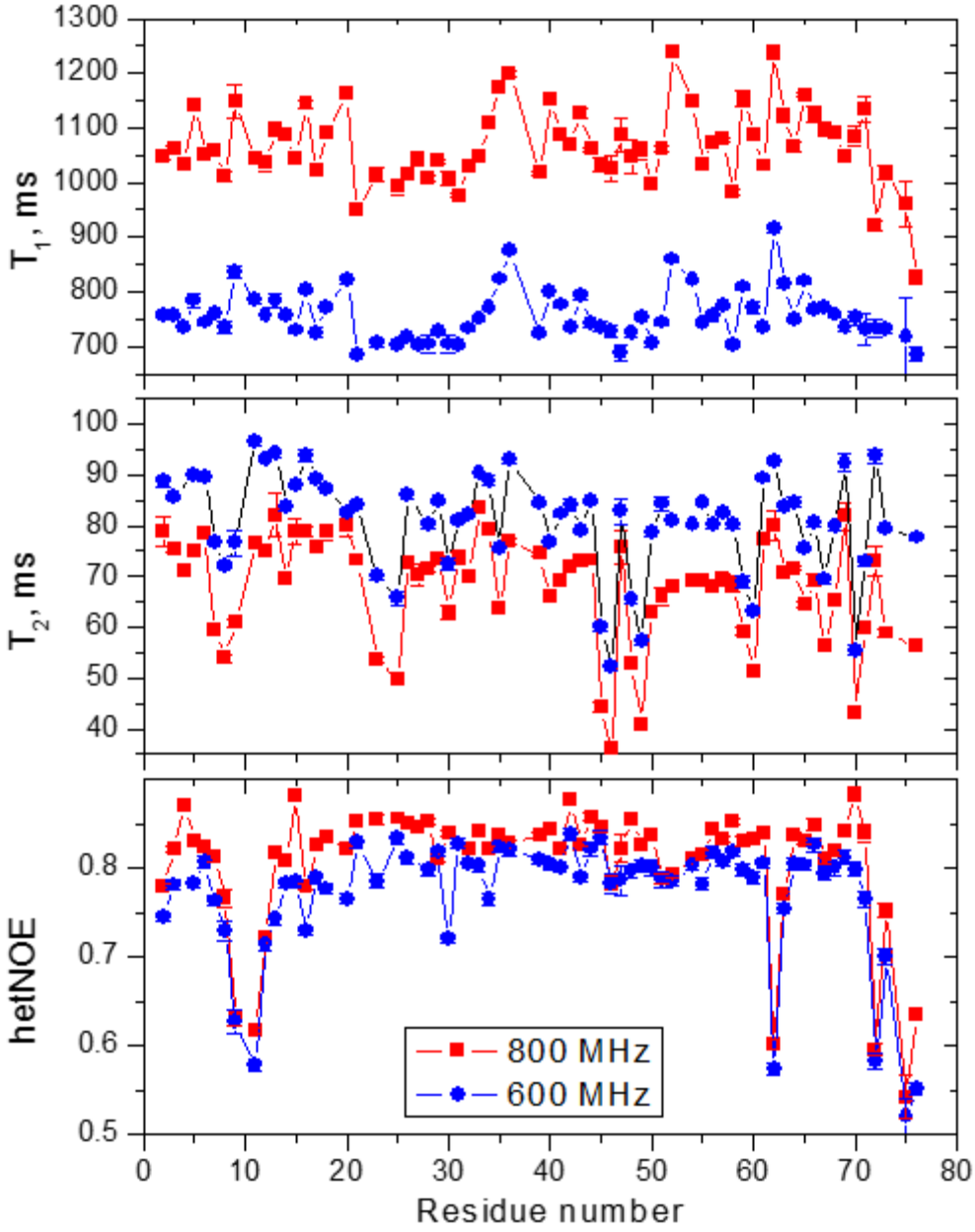

Figure 2-6: 15N Relaxation data for backbone amides of cycUb2. Measurements were taken using 800 MHz (red) and 600 MHz (blue).

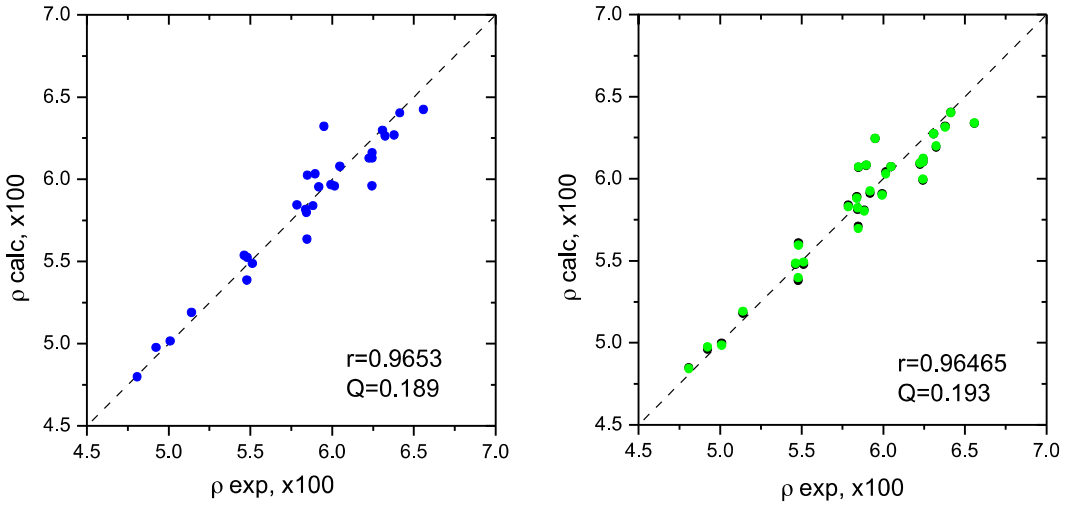

	D_x	D_y	D_z	α	β	γ	τ_c	r	Q	χ^2
1D3z_both	1.51(0.04)	1.62(0.03)	2.31(0.06)	90(3)	41(2)	89(11)	9.19(0.13)	0.96465	0.193	5.518
1D3z_D	1.50(0.06)	1.63(0.05)	2.31(0.07)	92(4)	42(3)	97(12)	9.19(0.18)	0.96532	0.189	5.327
1D3z_P	1.50(0.07)	1.63(0.05)	2.31(0.08)	88(4)	41(3)	82(14)	9.19(0.20)	0.9653	0.189	5.326
HYDRO	1.53	1.55	2.34				9.22			

Figure 2-7: ROTDIF analysis using relaxation data obtained from 600 MHz, taking into consideration either one domain (blue) or both domains (green).

2.5 Binding studies with cycUb$_2$

The crystal structure of cycUb$_2$ demonstrates that the two Ub domains are locked in a closed conformation in which the hydrophobic patch of each domain is sequestered at the interface. Several key hydrophobic residues generally involved in recognizing binding partners of Ub are buried from the surface in this structure. Solution NMR data is in agreement with the crystal structure, suggesting that cycUb$_2$ is locked in a closed conformation in solution as well.

If the hydrophobic patches necessary for binding are fixed in a buried position upon cyclization of K48-Ub_2, then it would seem that cyclization of K48-Ub_2 should hinder, if not abolish, its ability to interact with ligands. To test this, NMR titrations were performed using ligands with known affinities towards Ub or K48-Ub_2

2.5.1 UQ1-UBA

Ubiquilin-1 (UQ1) functions as a shuttle protein in the ubiquitin-proteasome system. It has a C-terminal UBA domain that binds to polyUb chains of substrates while its N-terminal UBL domain is recognized by the proteasome. The UBA domain of UQ1 is one of the tightest binders of Ub (K_d ~ 20 μM) and binds to K48-Ub_2 even tighter (K_d ~ 5 μM). The affinity of UQ1-UBA to polyUb is independent of linkage type; it should be able to bind Ub regardless of what kind of linkage it is involved in. UQ1-UBA acts as a receiver to the Ub "signal" in that it can recognize the canonical hydrophobic patch of Ub.

Unlabeled UQ1-UBA was titrated into ^{15}N cycUb_2 while a series of ^{1}H-^{15}N HMQC spectra were recorded at each titration point. Early in the titration ([UBA]/[cycUb_2] = 0.4-1.0), specific signal attenuations were observed for residues L8, R42, A46, G47, K48, Q49, L50, V70, L71, and L72. Residues T7 and G76 first shifted, then attenuated, and then finally reemerged in a new position at saturation throughout the course of the titration. These are examples of slow-intermediate exchange on the NMR timescale and certainly suggest that there is binding between UBA and cycUb_2. The titration was carried out until saturation ([UBA]/[cycUb_2] = 12.0), at which point CSPs

were calculated. Significant CSPs (>0.12) were observed for V5, T7, K11, T12, L15, Q41, L43, E51, L67, H68, L69, L73, and G76. Residues that were shifted or attenuated generally comprise the canonical hydrophobic patch of Ub (Figure 2-8). Despite the burial of hydrophobic residues in the structure of $cycUb_2$, the Ub "signal" is still recognizable by UQ1-UBA.

The stoichiometry of binding can be inferred from the T1 relaxation times of $cycUb_2$ before and after addition of ligand. Before adding ligand, $cycUb_2$ has an average T1 relaxation time of 760 ± 50 ms; at saturation the $cycUb_2$:UBA complex has an average T1 relaxation time of 1100 ± 100 ms. This seems to indicate that the stoichiometry between $cycUb_2$ and UBA is 1:2, as a T1 relaxation time of 1100 ± 100 ms corresponds to a protein complex with an estimated size of 30.4 ± 3.1 kDa. Furthermore, upon addition of ligand to ^{15}N $cycUb_2$, only one set of peaks remained. This may suggest that the complex maintained symmetry, which would likely not be the case if the binding were 1:1. However, ignoring the T1 relaxation data that clearly suggests 1:2 stoichiometry, and solely taking into consideration the observation of one set of peaks, 1:1 binding is possible if the complex exists as an ensemble of multiple conformations that interconvert in the fast exchange regime.

Assuming a stoichiometry of 1:2 ($cycUb_2$:UBA), a dissociation constant (K_d) of 280 ± 70 µM was calculated from the CSPs from each point in the titration (Figure 2-9). This suggests that UQ1-UBA has a much lower affinity than it does for either monoUb or acyclic $K48Ub_2$.

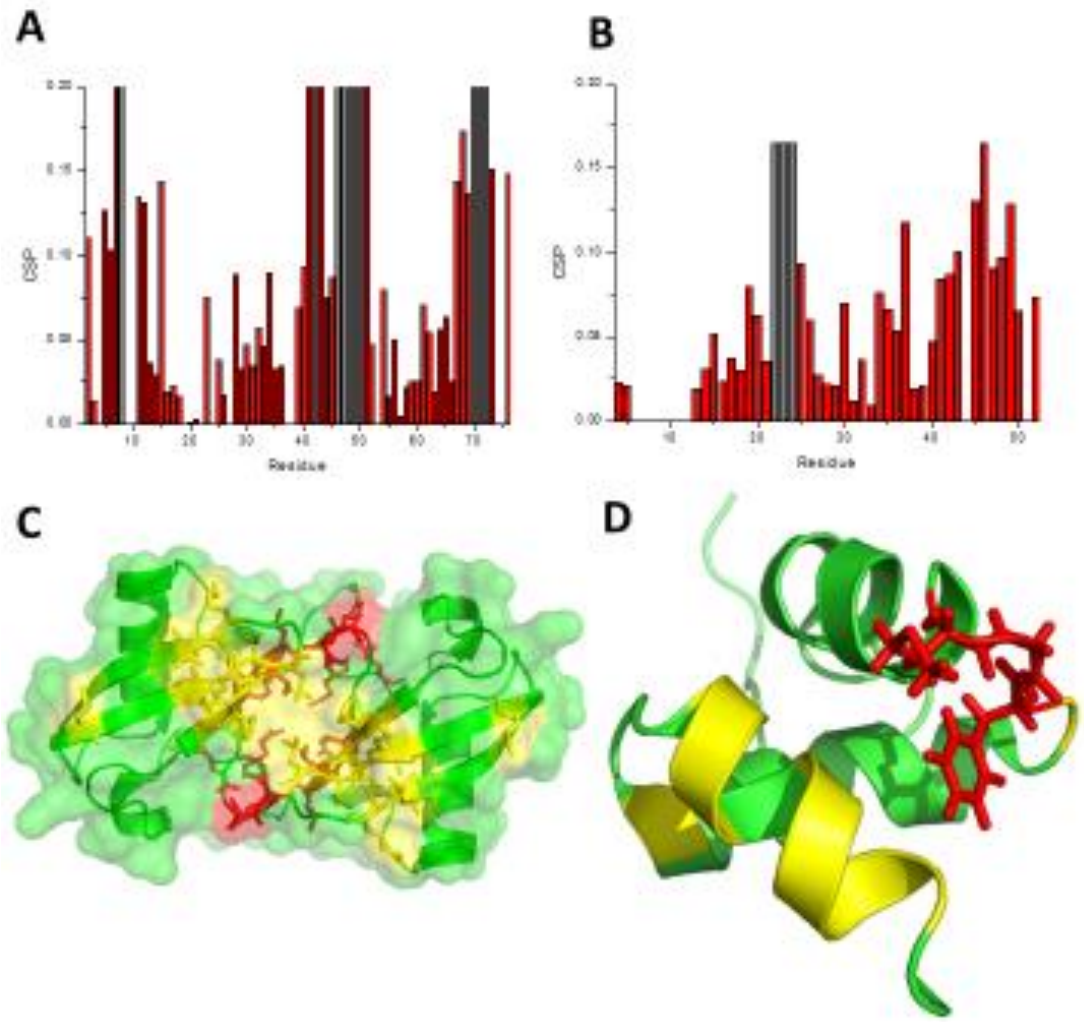

Figure 2-8: NMR titrations of 15N cycUb$_2$ with unlabeled UQ1-UBA and vice versa. A: CSP plot of cycUb$_2$ at saturation (1:12) with UQ1-UBA. B: CSP plot of UQ1-UBA at saturation (1:3) with cycUb$_2$. Gray bars represent attenuations. C: CSPs (>0.08, yellow) and attenuations (red) mapped on the surface of cycUb$_2$ crystal structure. D: CSPs (>0.08, yellow) and attenuations (red) mapped on the surface of UQ1-UBA crystal structure.

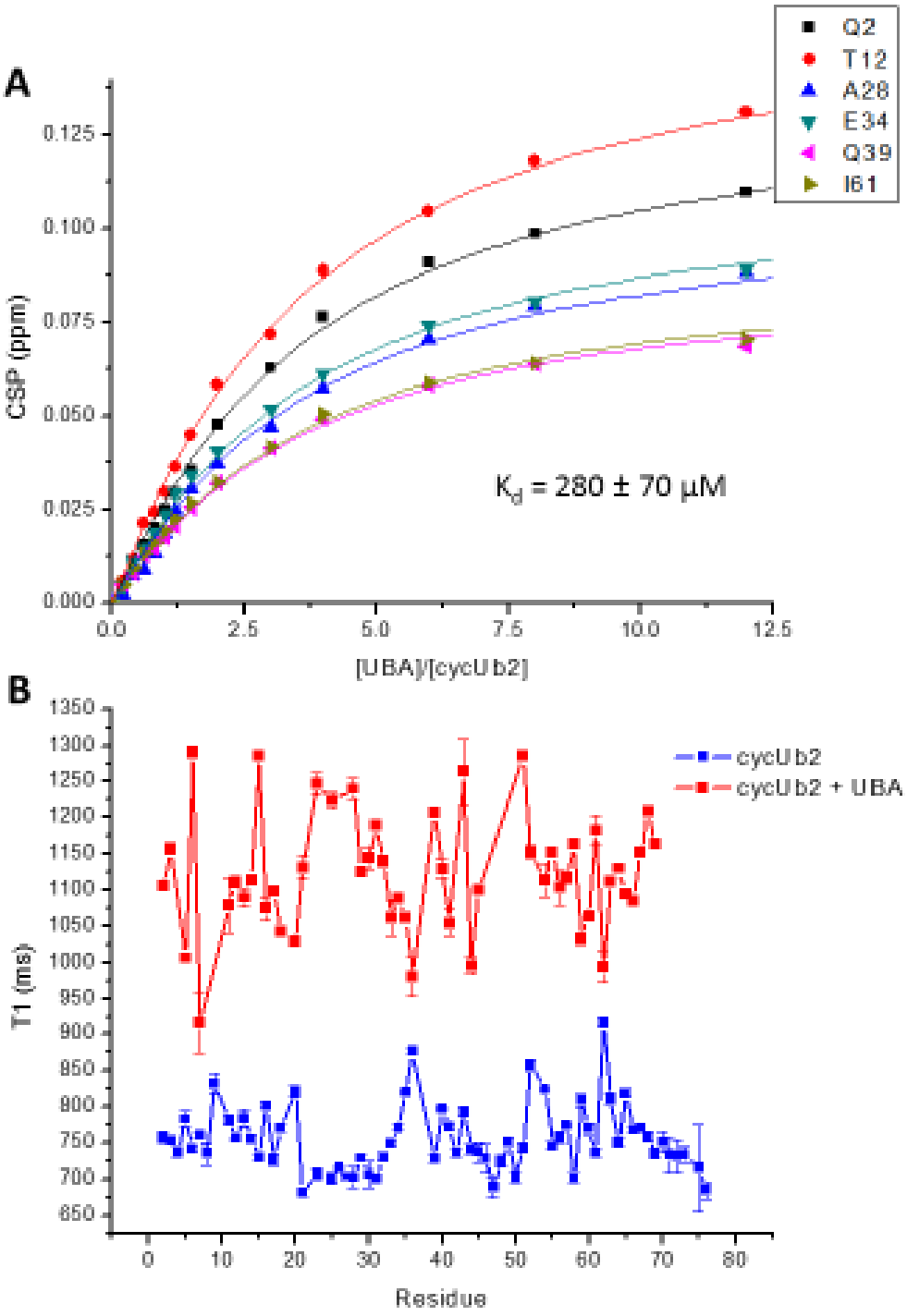

Figure 2-9: Titration of 15N cycUb$_2$ with unlabeled UQ1-UBA. A: Plot of CSP vs [UBA]/[cycUb$_2$] ratio for residues selected in calculation of K_d. B: Plot of T1 relaxation for cycUb$_2$ in the presence and absence of UQ1-UBA at saturation.

2.5.2 hHR23a-UBA2

The human homolog of Rad23a (hHR23a) is another example of an UBL-UBA shuttle protein as it is able to bind both Ub chains as well as the 26S proteasome. hHR23a has one N-terminal UBL domain and two UBA domains, UBA1 and UBA2. Previous studies using the minimal UBA2 domain have demonstrated that it binds Ub chains in a length-dependent manner and that it binds preferentially to K48-linked polyUb chains. UBA2 has a higher affinity towards K48-Ub_2 than monoUb, and binds tighter to the proximal domain (18μM for proximal, 140μM for distal, 400μM for monomer). Upon binding to K48-Ub_2, at low [UBA2]/[K48-Ub_2] ratios, UBA2 interacts with hydrophobic patches of both Ub domains simultaneously in a "sandwich-like mode"[25]. This mode of interaction is believed to contribute to the specificity of UBA2 binding preferentially to K48-linked chains.

Given that UBA2 is a linkage-specific receptor of K48-Ub_2, we wanted to see if and how UBA2 would interact with cycUb_2. To test if UBA2 can recognize cycUb_2, unlabeled UBA2 was titrated into ^{15}N cycUb_2. Signal attenuations were first observed at a [UBA2]/[cycUb_2] ratio of 1:1 for the following residues: T7, R42, I44, A46, G47, K48, Q49, L50, H68, V70, L71, R72, L73, G75. The peak for G76 shifted, attenuated, and reappeared at saturation (1:12). Significant CSPs (>0.1) were observed for T9, T14, E51, and G76 (Figure 2-10). For the residues of cycUb_2 involved in the interaction with UBA2, the majority of them are in slow-intermediate exchange. Those

that were in fast exchange were used to determine a K_d of 240 ± 40 µM assuming 1:2 ($cycUb_2$:UBA2) stoichiometry (Figure 2-11). T1 relaxation times determined for $cycUb_2$ before (760 ± 50 ms) and after (1100 ± 100 ms) saturation with UBA2 suggest that the final complex at saturation has an overall size of roughly 30 kDa.

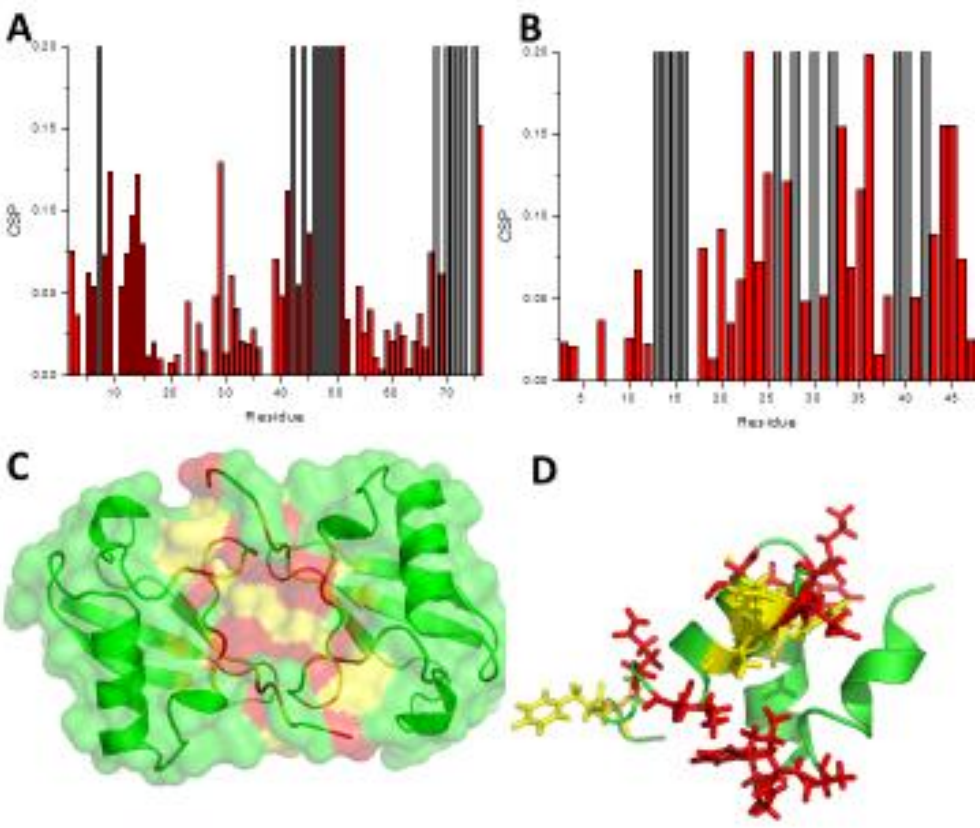

Figure 2-10: NMR titrations of 15N $cycUb_2$ with unlabeled UBA2 and vice versa. A: CSP plot of $cycUb_2$ at saturation (1:12) with UBA2. B: CSP plot of UBA2 at saturation (1:2) with $cycUb_2$. Gray bars represent attenuations. C: CSPs (>0.08, yellow) and attenuations (red) mapped on the surface of $cycUb_2$ crystal structure. D: CSPs (>0.08, yellow) and attenuations (red) mapped on the surface of UBA2 crystal structure.

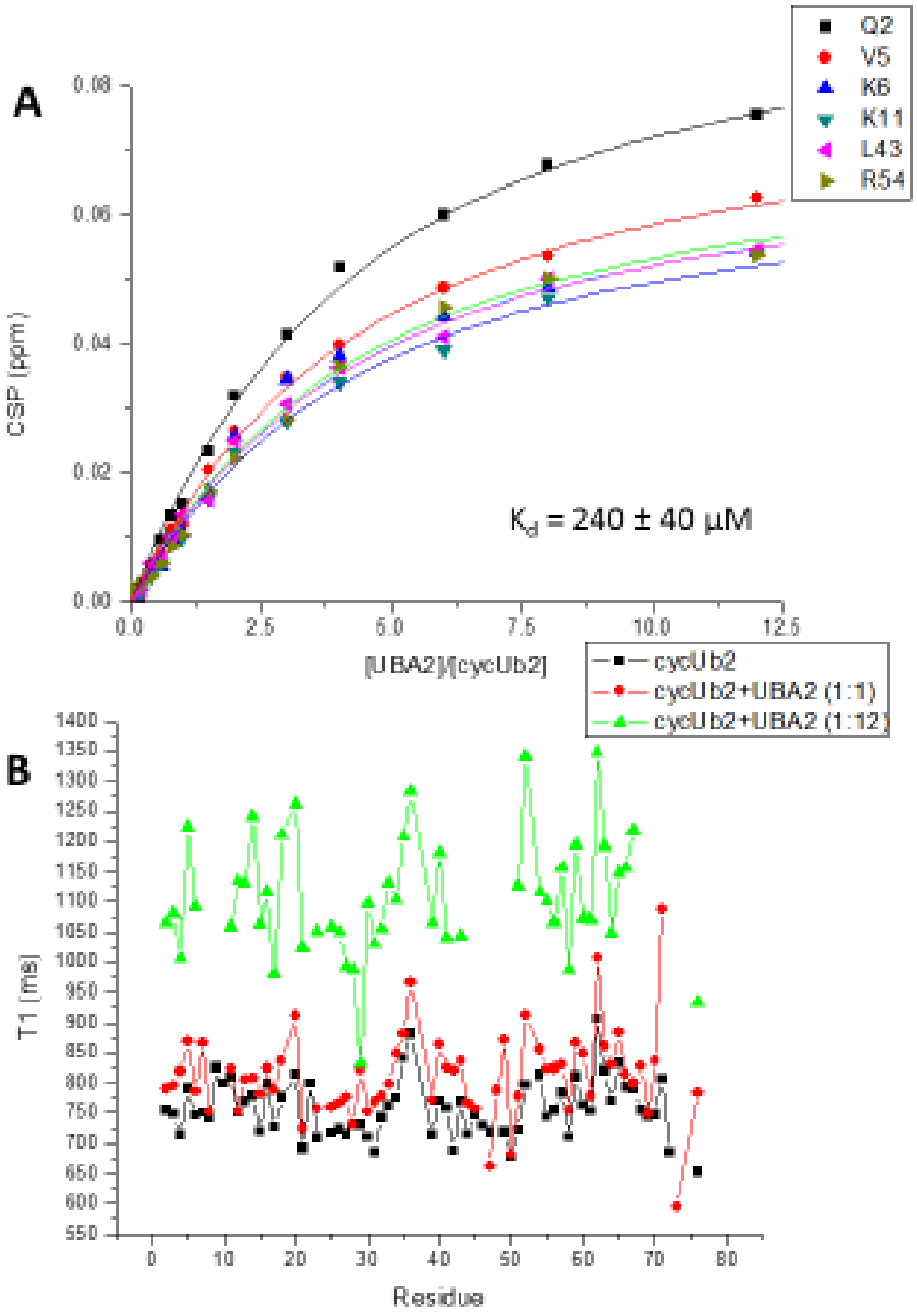

Figure 2-11: Titration of 15N cycUb$_2$ with unlabeled UBA2. A: Plot of CSP vs [UBA2]/[cycUb$_2$] ratio for residues selected in calculation of K_d. B: Plot of T1 relaxation for cycUb$_2$ in the presence and absence of UBA2 at 1:1 and at saturation.

2.5.3 Rpn10-UIM

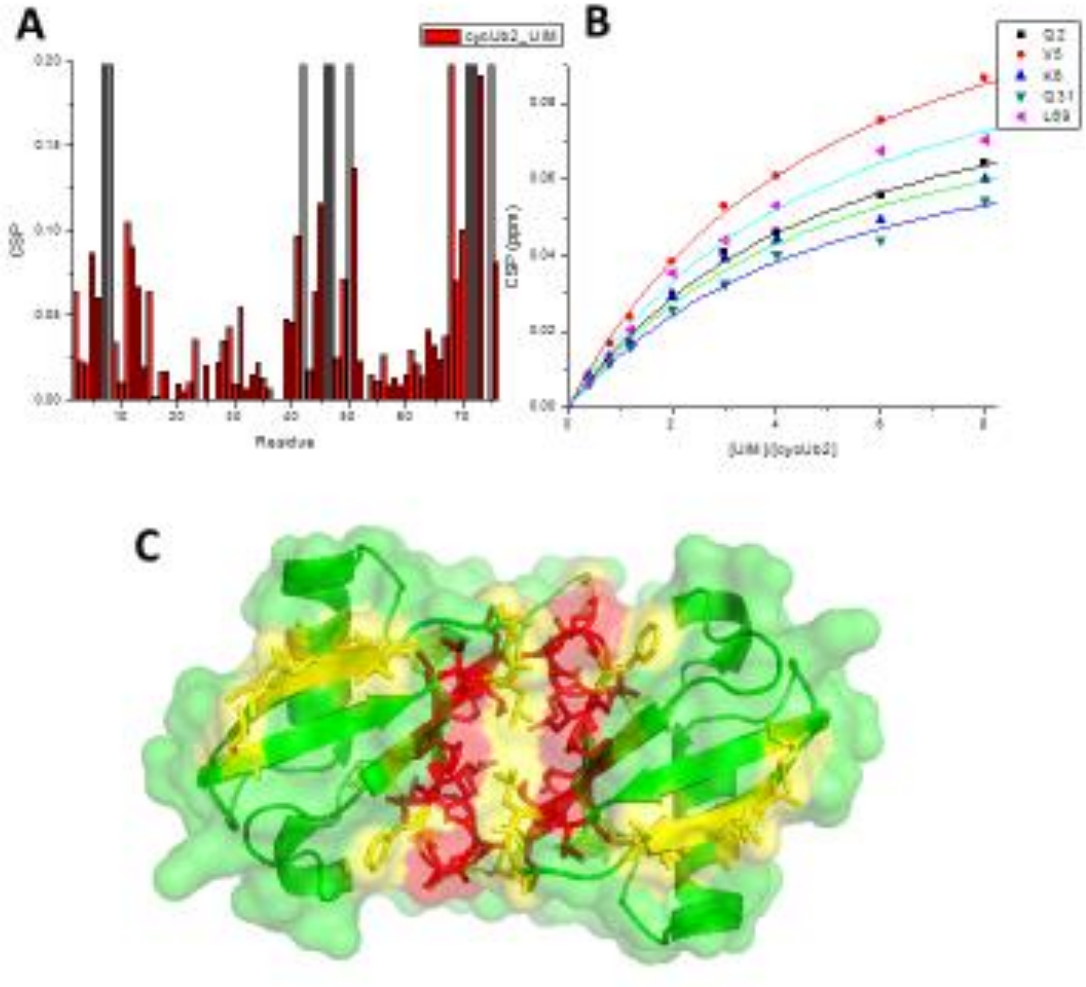

Figure 2-12: NMR titration of 15N cycUb$_2$ with Rpn10-UIM. A: CSP plot of cycUb$_2$ nearly at saturation (1:8) with Rpn10-UIM. B: Plot of CSP vs. [UIM]/[cycUb$_2$] ratio for residues selected in calculation of K_d. C: CSPs (>0.08, yellow) and attenuations (red) mapped on the surface of cycUb$_2$ crystal structure.

NMR Titrations				
^{15}N-P	L	$[P]_0$ (μM)	K_d (μM)	Stoichiometry
$cycUb_2$	UQ1_UBA	100	280 ± 70	1:2
$cycUb_2$	hHR23a_UBA2	70	240 ± 40	1:2
$cycUb_2$	Rpn10_UIM	100	460 ± 110	1:2
UBA	$cycUb_2$	200	1000 ± 300	2:1
UBA2	$cycUb_2$	200	250 ± 70	2:1

Table 2-2: Summary of NMR titrations. ^{15}N-P stands for the isotopically labeled protein, L stands for ligand, $[P]_0$ is the initial concentration of labeled protein, and K_d is the apparent dissociation constant assuming stoichiometries as shown.

2.5.4 HyTEMPO

HyTEMPO is a small paramagnetic molecule that is known to bind to the hydrophobic patch on Ub surface. Previous studies have shown that it preferentially binds, or binds tighter to, K48-Ub_2 over monoUb[21]. Upon binding, HyTEMPO introduces a paramagnetic effect to residues in proximity to its paramagnetic center. In comparison to Ub, more attenuations and stronger attenuations are observed upon binding of HyTEMPO to K48-Ub_2. If we map the residues involved in the binding of HyTEMPO to K48-Ub_2 onto the crystal structure of $cycUb_2$ we find that most of the residues involved are buried (Figure 2-13). The previous finding that K48-Ub_2 is preferred over monoUb is reproduced. $CycUb_2$ has a nearly identical ratio intensity profile to K48-Ub_2 (distal).

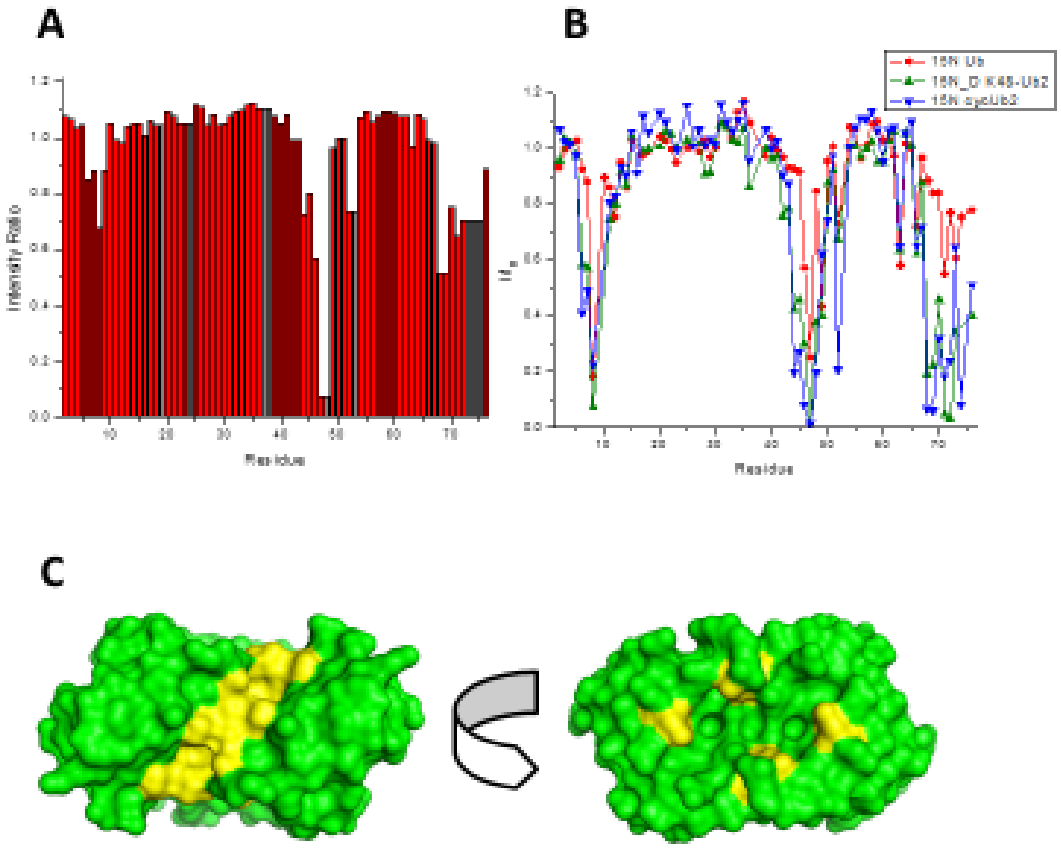

Figure 2-13: Solvent accessibility of hydrophobic patch of cycUb$_2$. Attenuation of signal intensity observed upon incubation with a hydrophobic paramagnetic molecule (HyTEMPO). A: Plot of intensity ratios (I/I_0) observed for each backbone amide of cycUb$_2$ upon addition of HyTEMPO at 20 times molar excess. B: Comparison of intensity ratio plots for Ub, K48-Ub$_2$ (distal), and cycUb$_2$ upon addition of HyTEMPO (1:20). C: Significantly attenuated residues ($I/I_0 < 0.6$, yellow) mapped on the surface of cycUb$_2$ (green).

2.6 pH titration of cycUb$_2$

The equilibrium between open and closed conformations of K48-Ub$_2$ is pH-dependent[21]. At neutral or high pH, significant CSPs (>0.2) are observed for residues that comprise the hydrophobic interface, whereas at low pH, these residues have relatively lower CSPs (<0.05). Generally, this indicates a shift toward the open conformation as pH decreases.

The second isopeptide bond of cycUb$_2$ restricts the range of conformations that it may take. To observe the effect of pH on the conformational equilibrium of cycUb$_2$, a solution containing ^{15}N cycUb$_2$ was titrated from pH 4.4 to 7.6 in sodium phosphate/acetic acid buffer. HMQC (SOFAST) spectra were collected at pH 4.4, 5.2, 6.0, 6.8, and 7.6. Spectra were collected for ^{15}N Ub in the same buffer conditions as cycUb$_2$ at each pH to determine CSPs.

As the pH increases, so do the magnitudes of the CSPs, generally centered at the canonical hydrophobic patch of Leu8, Ile44, and Val70 (Figure 2-14). This phenomenon is also observed in K48-Ub$_2$ in that as the buffer becomes more basic, the dimer adopts a more closed conformation on average. In other words, if we are to assume a two-state model, the equilibrium between open and closed states shifts towards the closed state. However, in the case of K48-Ub$_2$, there are virtually no CSPs observed at low pH except for directly around the site of the isopeptide linkage. For cycUb$_2$ there are still significant perturbations around the hydrophobic patch even at low pH. This demonstrates that cycUb$_2$ undergoes a shift in its conformational equilibrium as pH is increased, and that cycUb$_2$ cannot completely open at low pH in contrast to what was observed for K48-Ub$_2$.

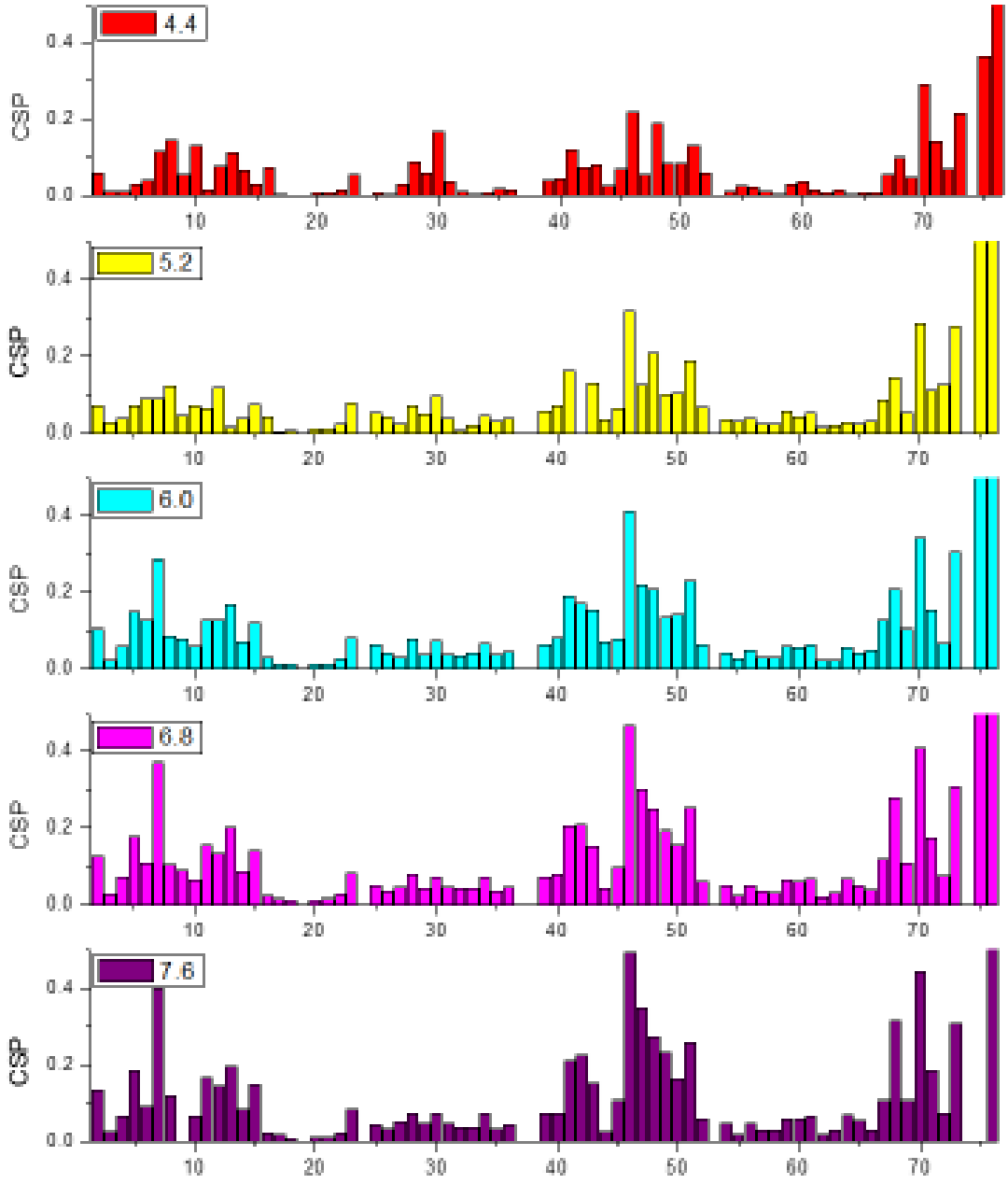

Figure 2-14: Effect of pH on CSPs observed for cycUb$_2$. CSP plots comparing ^{1}H-^{15}N HSQC spectra of cycUb$_2$ and Ub in 20 mM phosphate/citric acid buffer at various pH (4.4, 5.2, 6.0, 6.8, and 7.6).

2.7 SANS

Small angle neutron scattering (SANS) can provide information about the overall shape of a protein. SANS data were collected for $cycUb_2$ at NIST Center for Neutron Research. Scattering profiles (I(q)) and atom pair distribution functions (P(r)) of $cycUb_2$ and K48-Ub_2 have distinct features (Figure 2-15). The P(r) vs. r plot of $cycUb_2$ has a distribution centered on r = 20Å, whereas that of K48-Ub_2 has a noticeable "hump". In comparison to K48-Ub_2, $cycUb_2$ has relatively more atom pair distances between 25-35Å and relatively less atom pair distances greater than 35Å. This is indicative of K48-Ub_2 adopting a more open structure and that the two Ub domains are likely further apart on average.

Predicted P(r) from the crystal structure of $cycUb_2$ has a narrower distribution, and therefore a more compact structure than what is observed in solution. Perhaps there are some dynamic properties of $cycUb_2$ in solution (opening/closing) to explain this discrepancy.

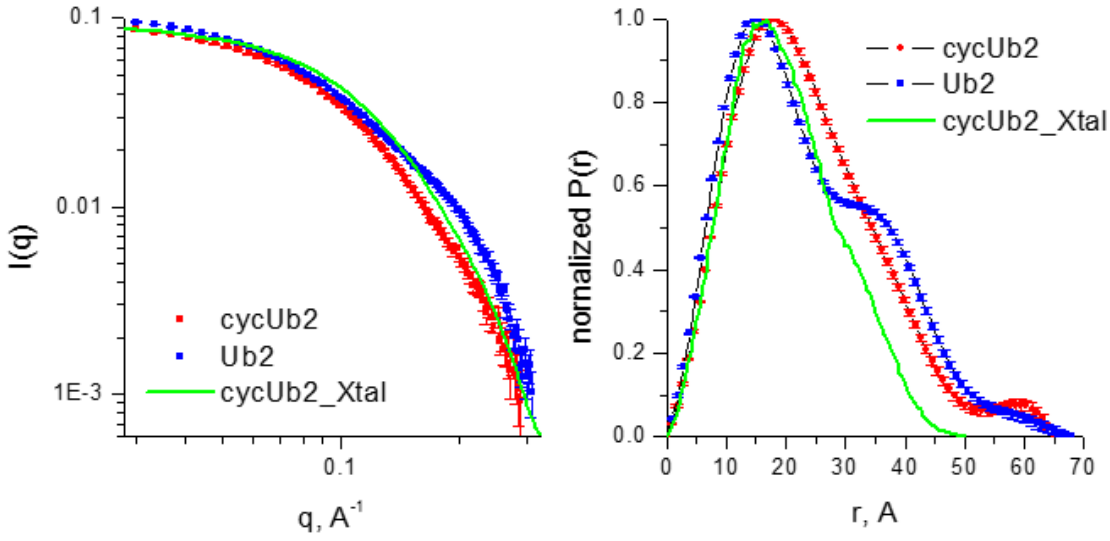

Figure 2-15: Experimental SANS data of cycUb$_2$. I(q) and P(r) plots shown for cycUb$_2$ (red) and K48-Ub$_2$ (blue). Error bars represent the combined standard uncertainty of the data collection. Back-calculated I(q) and P(r) plots from crystal structure of cycUb$_2$ (green).

2.8 DUB assays

Since there is evidence for the existence of cycUb$_2$ *in vivo*, it is important to consider how the cell disassembles cycUb$_2$. It can be assumed that the cell does have a mechanism to recycle cycUb$_2$ because otherwise there would be an uncontrolled accumulation of cyclic chains. Generally, ubiquitin chains are cleaved at the isopeptide linkage by specific proteases known as deubiquitinases (DUBs), resulting in the production of free monoUb (or smaller Ub chains).

DUBs act on different mechanisms and vary in terms of linkage-specificity and mode of interaction between the active site and the region immediately surrounding the isopeptide linkage of a polyUb chain. In the purification of cycUb$_2$,

isoT (USP5) is used to selectively cleave acyclic chains since it has been shown that isoT requires the presence of a free C-terminus in order to recognize and cleave Ub chains. Therefore, as expected, isoT specifically disassembled acyclic chains into Ub monomers, leaving the cyclized products untouched.

Six different DUBs were tested for their activity with $cycUb_2$ as the substrate. Of these DUBs, Cezanne and AMSH do not cleave K48-linked chains as they are K11- and K63-specific respectively. The other four DUBs: OTUB1, Ubp6, USP2, and USP5 (isoT) are capable of cleaving K48-linked chains. As explained earlier, USP5 is not expected to have any DUB activity with $cycUb_2$ due to its lack of free C-terminus.

Interestingly, of the DUBs tested, OTUB1 was able to, very slowly, cleave $cycUb_2$ (Figure 2-16). While the kinetics of the reaction were not determined, the rate of reaction is markedly slower than for the acyclic form of K48-Ub_2. Some $cycUb_2$ still remains after incubation with OTUB1 at 30°C for 16h at a molar ratio of 10:1. Under the same conditions, a sample of K48-Ub_2 would be completely degraded within minutes.

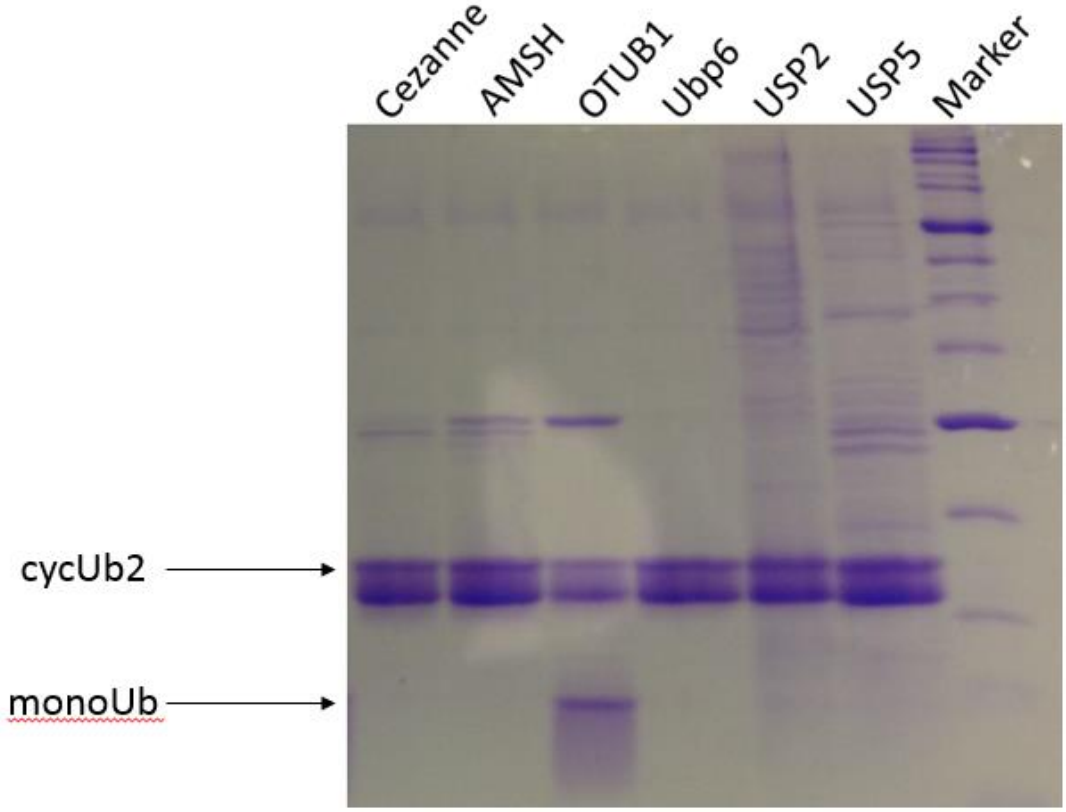

Figure 2-16: Assay of deubiquitinase activity of various DUBs (Cezanne, AMSH, OTUB1, Ubp6, USP2, and USP5 (isoT)) on $cycUb_2$ in a buffer containing 50 mM Tris pH 8.0, incubated at 30°C for 16h, with a 10:1 molar ratio between $cycUb_2$ and DUB. Coomassie stained 15% SDS-PAGE gel; pure $cycUb_2$ naturally runs as two bands; appearance of monoUb observed upon addition of OTUB1. Purified proteins used in DUB assay shown in Appendix (Figure A-6).

Chapter 3: Structural and Biochemical Studies of $cycUb_3$

3.1 Introduction

Cyclic forms of free K48-linked polyUb chains of varying lengths ($n \geq 2$) are generated by *in vitro* ubiquitination reactions catalyzed by the conjugating enzyme E2-25k. As detailed in Chapter 2, $cycUb_2$ was created and isolated for use in structural, dynamical, and biochemical analysis. Through the same purification steps used to isolate $cycUb_2$, cyclic K48-linked tri-ubiquitin ($cycUb_3$) can be isolated as well. Until now not much is known about the properties of $cycUb_3$. In fact, there are no structures of any Ub_3 in the Protein Data Bank. This presents us with the unique opportunity of determining the first known structure of Ub_3.

3.2 Crystal Structure of $cycUb_3$

As detailed in Chapter 2.3, a highly pure sample of $cycUb_2$ was prepared and subject to crystal screening. After a round of optimization, crystals suitable for X-ray diffraction grew under different conditions varying in pH, precipitant concentration, and buffer composition. Likewise, a highly pure sample of $cycUb_3$ ultimately yielded useful crystals for X-ray crystallography. The protein structure was determined by Dr. Paul Paukstelis and refined to a resolution of 1.65Å. Surprisingly, the crystal structure of $cycUb_3$ is asymmetrical despite that each Ub domain should be indistinguishable from one another. A compact hydrophobic interface between the Ub domains is not

observed as was in $cycUb_2$; the structure of $cycUb_3$ is relatively more open with its hydrophobic patches exposed (Figure 3-1).

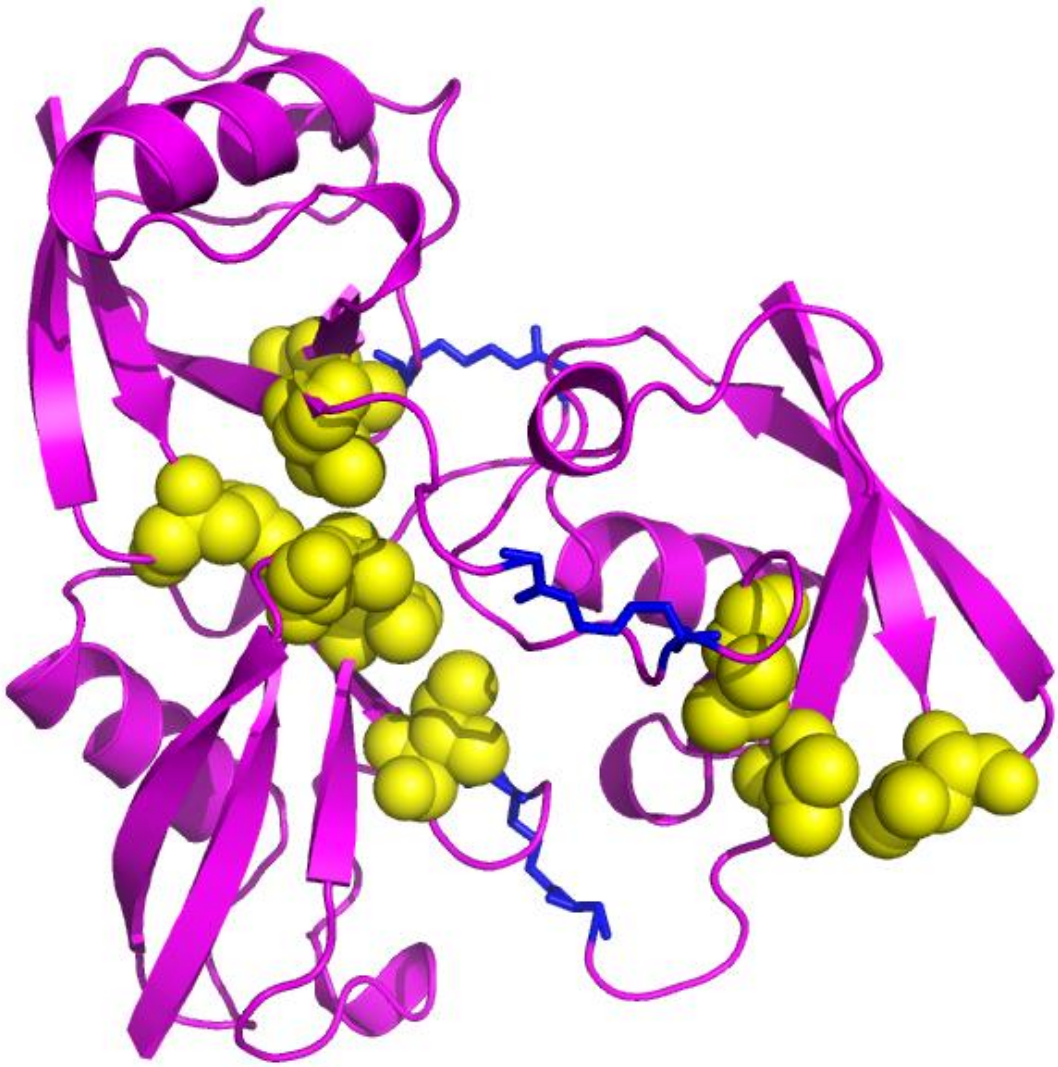

Figure 3-1: Crystal structure of cycUb3. Residues involved in isopeptide linkages (K48, G76) shown as blue sticks, canonical hydrophobic patch (L8, I44, V70) shown as yellow spheres.

Resolution range (Å)	41.663 – 1.652
Total reflections	49813
Completeness (%)	99.94
Wilson B-factor	None
R-work	0.1873
R-free	0.2143
Number of non-hydrogen atoms	4217
water	646
Protein residues	456
RMS(bonds)	0.006
RMS(angles)	0.956
Ramachandran favored (%)	100
Ramachandran allowed (%)	0
Ramachandran outliers (%)	0
Clashscore	3.16

Table 3-1: Data collection statistics of cycUb$_3$ crystal.

3.3 Characterization of cycUb$_3$ in solution by NMR

3.3.1 HMQC experiment

As observed for cycUb$_2$, a ^{1}H-^{15}N HMQC spectrum of isotopically labeled ^{15}N cycUb$_3$ only has one set of chemical shifts corresponding to its backbone amide protons and nitrogens of all three Ub domains. By NMR, the three Ub domains are indistinguishable from one another, suggesting that the structure of cycUb$_3$ is symmetrical. However, the crystal structure obtained for cycUb$_3$ is asymmetrical, in which case one would expect to observe multiple sets of chemical shifts. It is possible that cycUb$_3$ does not adopt one symmetrical structure, but instead, exists as an ensemble of many possible orientations that quickly interconvert such that an average of all conformations is observed by NMR.

In general, the positions of the chemical shifts observed for $cycUb_3$ tend to lie on a linear path between the chemical shifts of monoUb and $cycUb_2$ (Figure 3-2), suggesting that $cycUb_3$ adopts a more open conformation than $cycUb_2$. In comparison to monoUb, the most highly perturbed chemical shifts are found around the residues that form the hydrophobic patch (Figure 3-3).

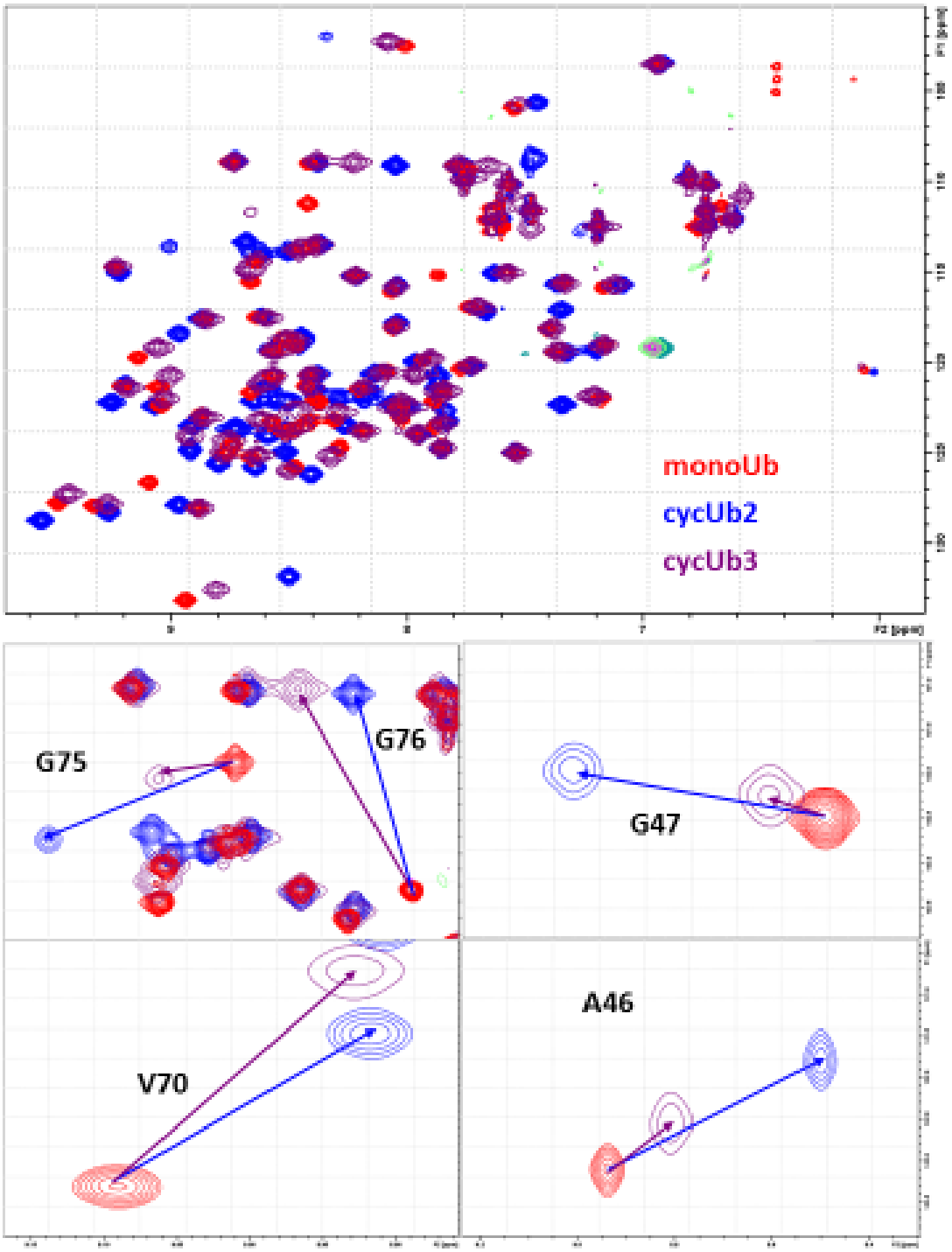

Figure 3-2: 1H-15N HMQC overlay of monoUb, cycUb2, and cycUb3 (red, blue, and magenta respectively). Areas of spectra are zoomed in around residues A46, G47, V70, G75, and G76; blue arrows from monoUb to $cycUb_2$; magenta arrows from monoUb to $cycUb_3$.

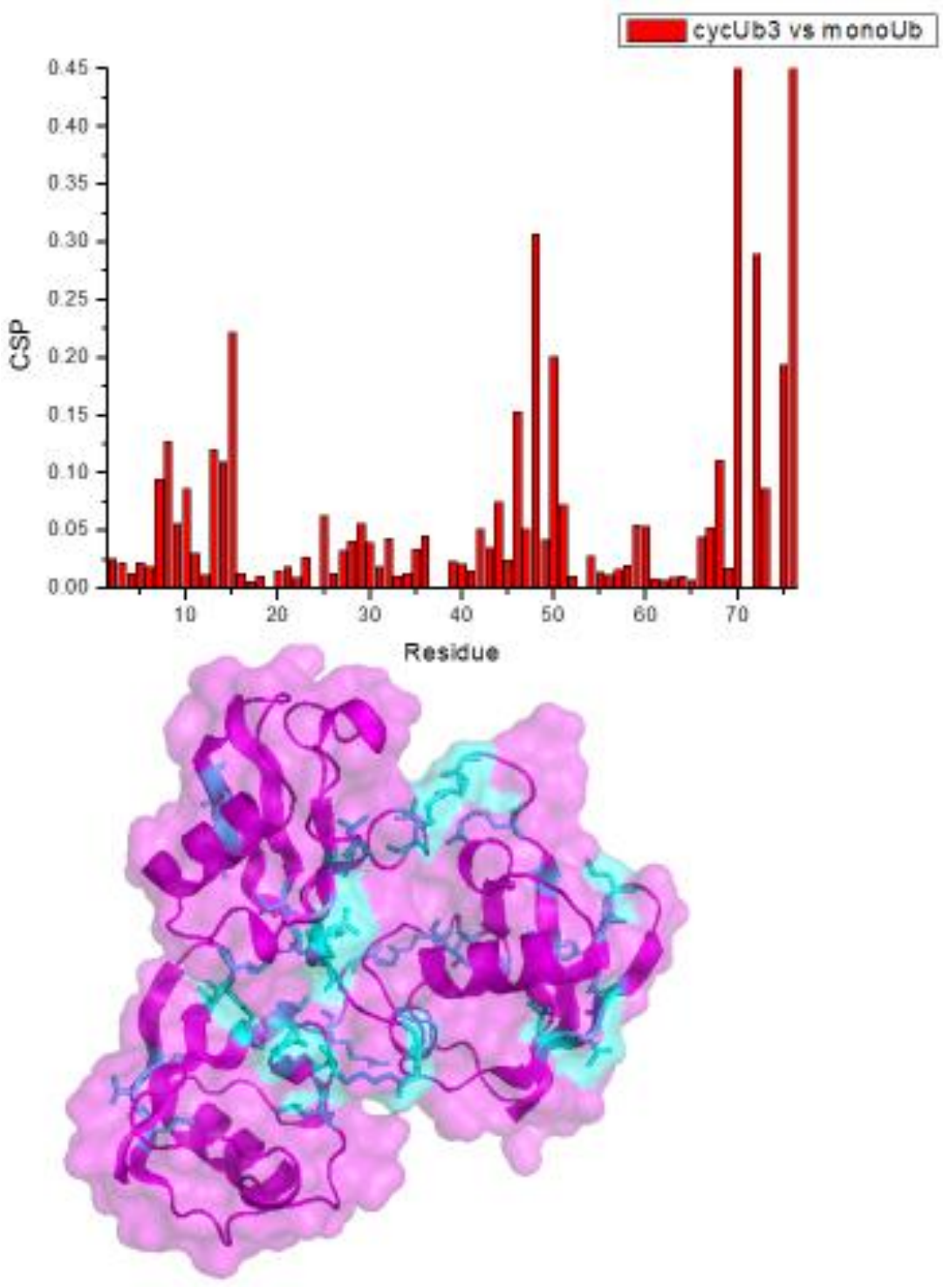

Figure 3-3: Chemical shift perturbations of cycUb3 in comparison to monoUb. CSP plot (top); CSPs greater than 0.1 ppm (cyan) mapped on the surface of the crystal structure of $cycUb_3$ (magenta).

3.3.2 ^{15}N Relaxation experiments

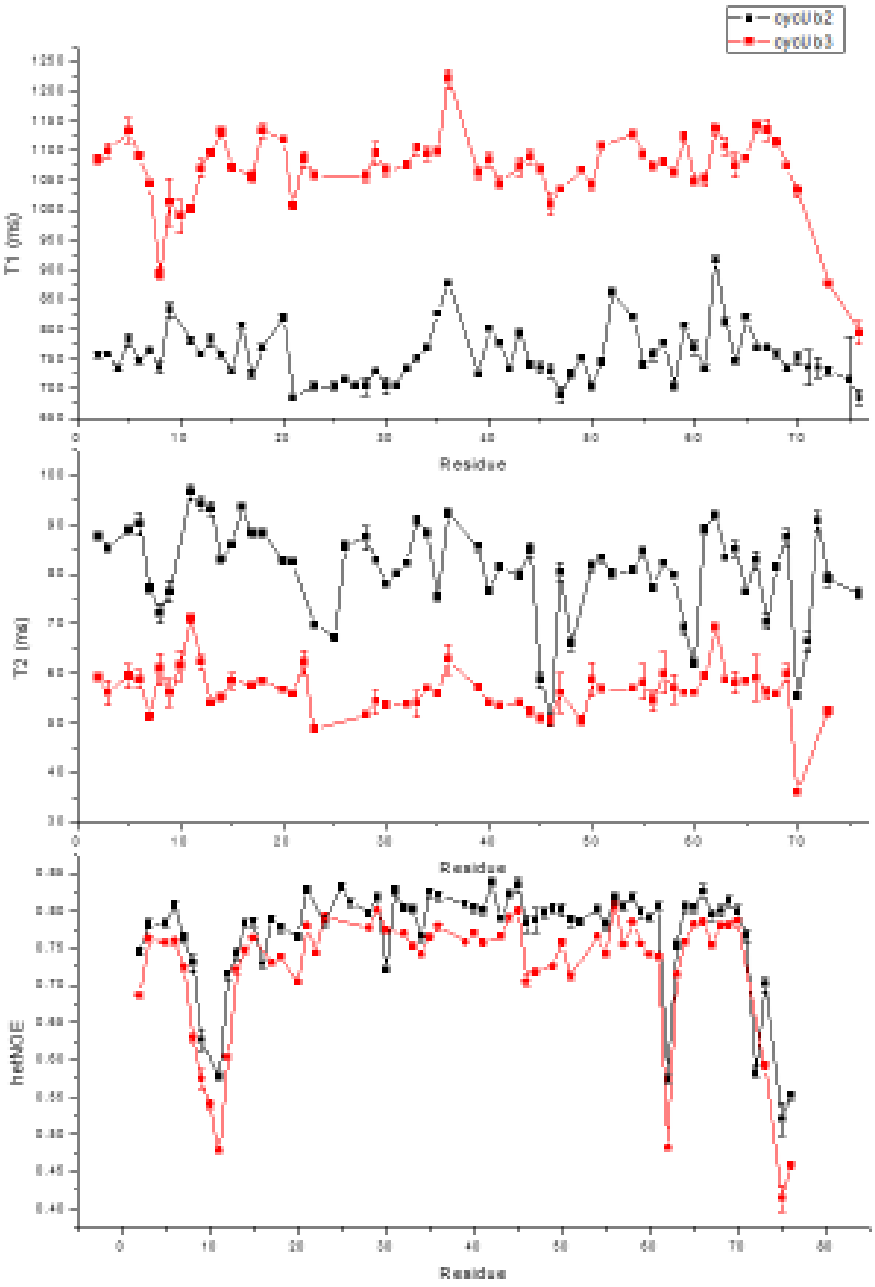

Figure 3-4: Relaxation data of ^{15}N cycUb$_3$ collected from Bruker 600 MHz NMR spectrometer. T1, T2, and heteronuclear data of cycUb$_2$ (black) overlaid with cycUb$_3$ (red).

3.3.3 pH titration of cycUb$_3$

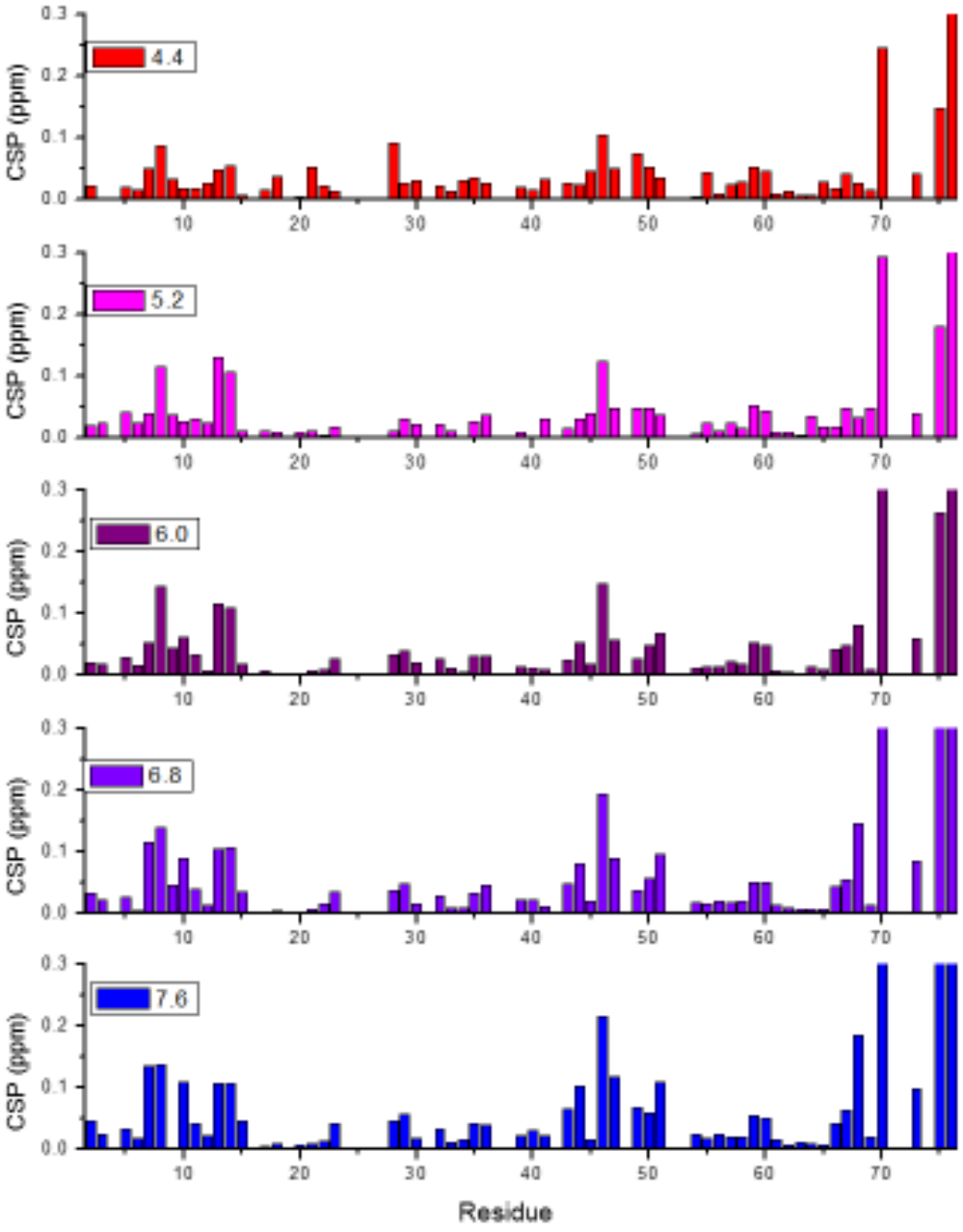

Figure 3-5: Effect of pH on CSPs observed for cycUb$_3$. CSP plots comparing ^{1}H-^{15}N HSQC spectra of cycUb$_3$ and Ub in 20 mM phosphate/citric acid buffer at various pH (4.4, 5.2, 6.0, 6.8, and 7.6).

3.4 NMR titration of UQ1-UBA into ^{15}N cycUb$_3$

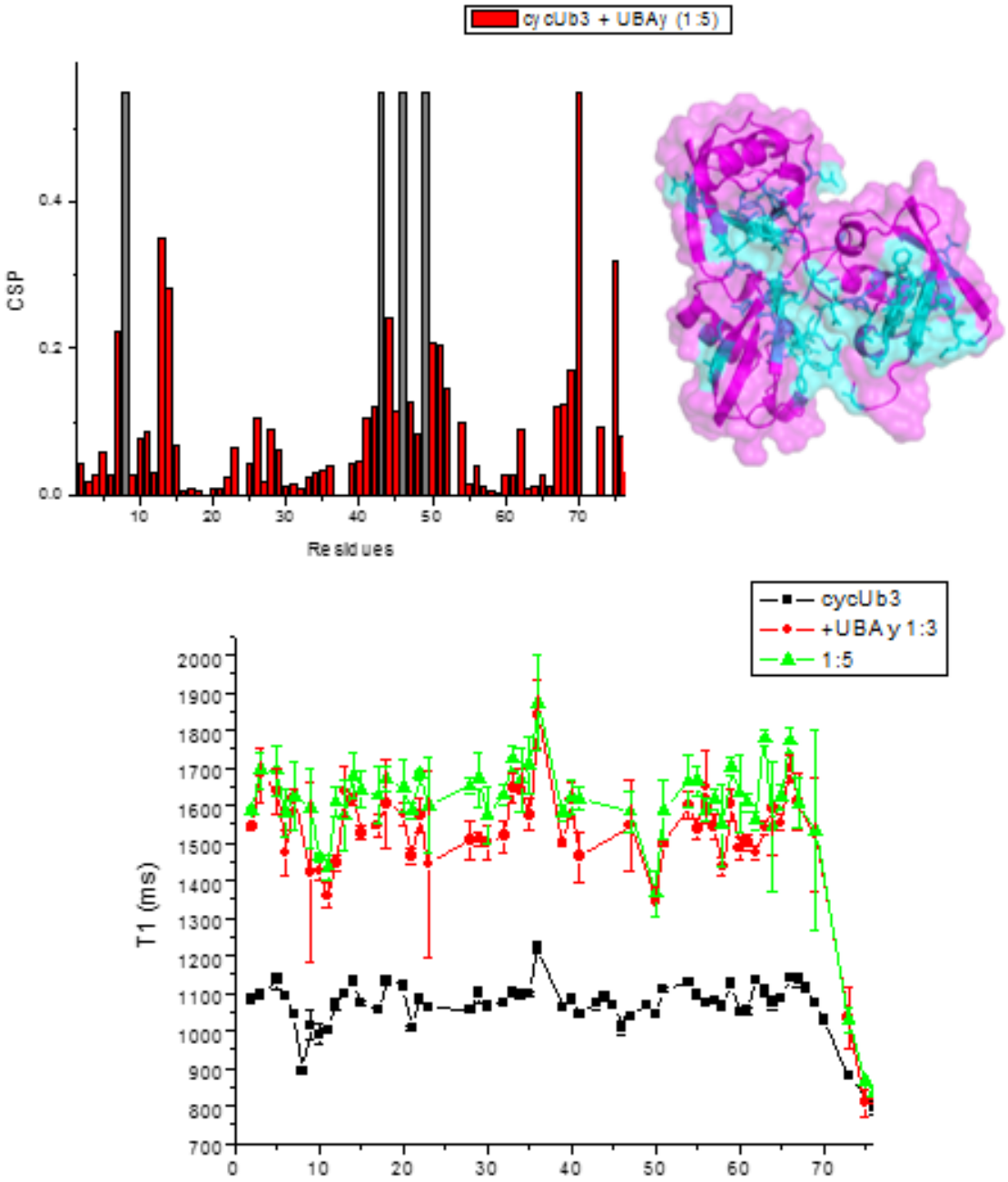

Figure 3-6: NMR titration of ^{15}N cycUb$_3$ with UQ1-UBA. CSP plot at saturation (1:5), gray bars represent attenuated residues. Residues with significant CSPs (>0.1, cyan) mapped on the surface of the crystal structure of cycUb$_3$ (magenta). T1 relaxation data for cycUb$_3$ before and after titration.

3.5 SANS

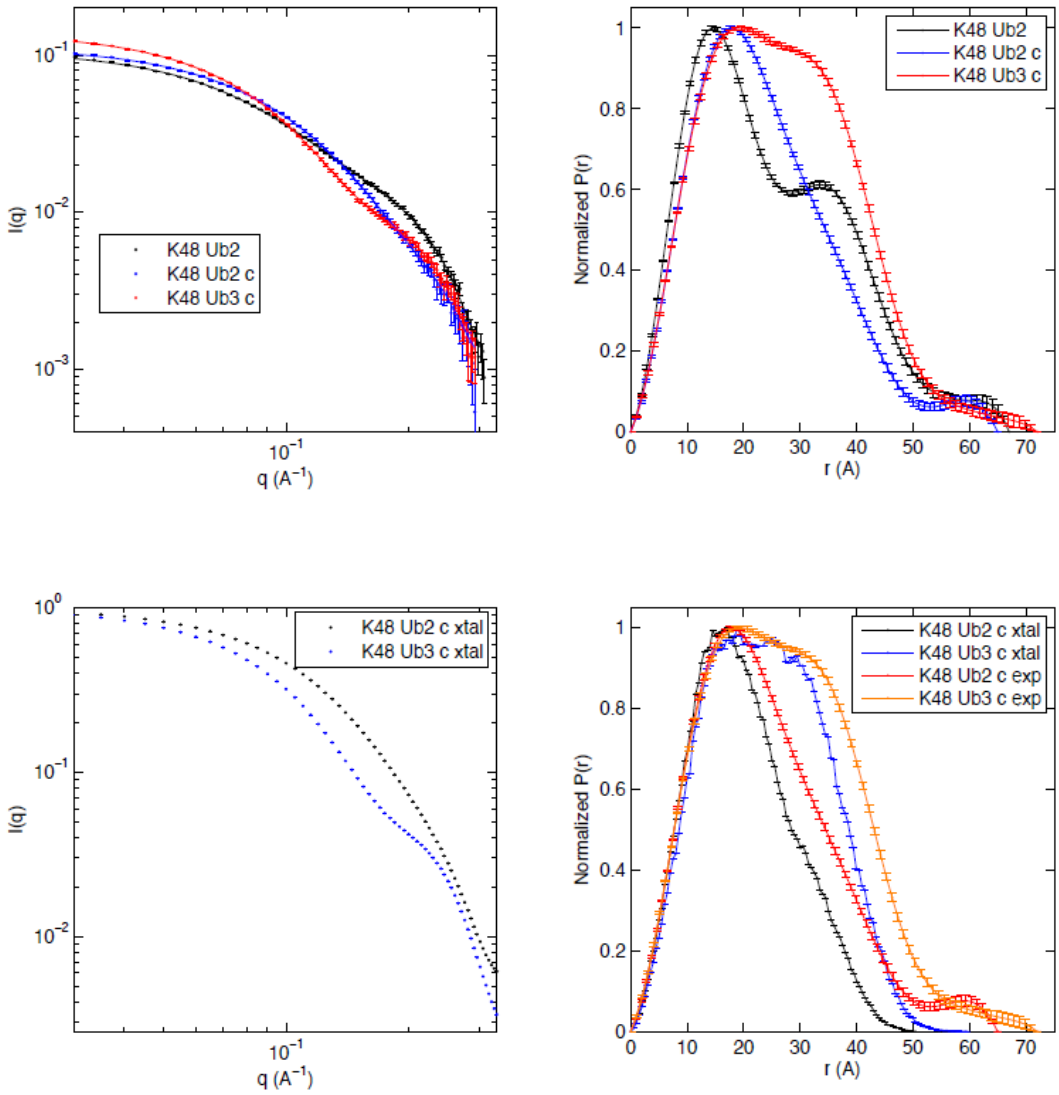

Figure 3-7: Experimental SANS data of cycUb$_3$. Top: I(q) and P(r) plots shown for K48-Ub$_2$ (black), cycUb$_2$ (blue), and cycUb$_3$ (red). Bottom: experimental SANS data for cycUb$_2$ and cycUb$_3$ in comparison to back-calculated data from crystal structures.

Chapter 4: Mechanistic insights into E2-25k mediated catalysis of K48-linked polyUb chains

4.1 Introduction

The Ub conjugating enzyme E2-25k catalyzes the formation of K48-linked polyubiquitin chains. The mechanism by which E2-25k works to specifically produce K48-linked polyubiquitin chains remains unclear. Recently, we obtained the crystal structure of E2-25k in complex with a K48-linked ubiquitin dimer. Each unit cell contains one ubiquitin and one E2-25k molecule where ubiquitin is non-covalently bound to the UBA domain by its well-studied hydrophobic patch. The crystal structure demonstrates that the distance between K48 of the acceptor ubiquitin, which is bound to the UBA domain, and the catalytic cysteine, C92, of E2-25k is roughly 40Å (Figure 1-2).

In order for a nucleophilic attack to occur, this distance needs to be approximately 5Å or lower. This strongly suggests that a conformational change may occur to bring the ε-amine group of K48 of the acceptor ubiquitin in closer proximity to the thioester Ub~E2-25k. Finding the mechanism by which E2-25k is able to catalyze the formation of polyubiquitin chains would increase our current understanding of ubiquitination and may serve as a model for other related mechanisms.

4.2 Formation of E2-25k disulfide

The E2-25k~Ub thioester intermediate is short-lived, making it difficult to study by NMR, so the thioester bond will be replaced with a disulfide bond for increased stability. The E2-25k~Ub disulfide complex was created by mixing E2-25k C170S and Ub G76C in the presence of $CuCl_2$ which acts as an oxidizing agent. The mutations were made to ensure that a disulfide bond would be created between the C-terminus of Ub and the catalytic cysteine (C92) of E2-25k, thus mimicking the thioester that naturally forms in the ubiquitination reaction. The formation of this disulfide was validated by non-reducing SDS-PAGE (Figure 4-1) and the complex was purified by size exclusion chromatography.

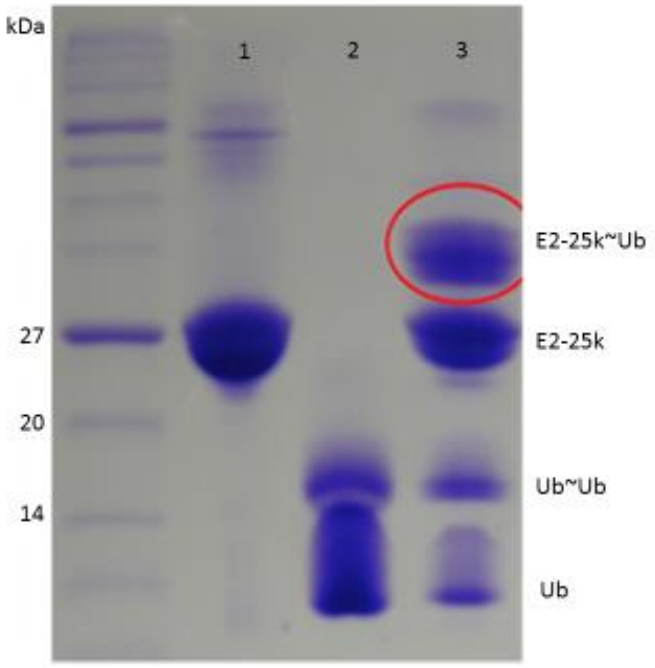

Figure 4-1: Non-reducing SDS-PAGE gel of E2-25k~Ub disulfide reaction. Protein marker (2-212 kDa); Lane 1, E2-25k C170S; Lane 2, Ub G76C; Lane 3, E2-25k~Ub disulfide circled in red.

4.3 NMR titration of E2-25k~Ub disulfide with Ub

Nuclear magnetic resonance (NMR) spectroscopy is very sensitive to the local chemical environment of the nuclei being observed; therefore it can be a very powerful tool to study protein-protein interactions. One specific method of studying such interactions would be to perform an NMR titration experiment while collecting ^{1}H-^{15}N HSQC spectra. HSQC spectra contain NMR signals (peaks) that mainly represent a correlation between backbone amide protons and nitrogens of the isotopically labeled (^{15}N) protein. Thus, after assignment of each peak to a specific residue, each residue of the protein can be studied individually.

Upon titration with an unlabeled protein, the chemical environment of interacting residues of the ^{15}N labeled protein changes, creating a shift in the position of these peaks. Such chemical shift perturbations (CSPs) provide information on which residues of the isotopically labeled protein are affected by the interaction with the unlabeled protein. These residues can be mapped on the surface of the protein being observed.

4.3.1 Titration of E2-25k~Ub into ^{15}N Ub

Bacterially expressed Ub was grown in minimal media in which the sole nitrogen source was ^{15}N labeled NH_4Cl, ensuring the incorporation of ^{15}N in the cellular synthesis of Ub. After purification, an NMR sample of ^{15}N Ub was prepared at a concentration of 200 µM. Unlabeled E2-25k~Ub disulfide was titrated into the solution of ^{15}N Ub while ^{1}H-^{15}N HSQC spectra were collected at each titration point. As a control, the same titration was performed by adding C170S E2-25k into ^{15}N Ub. CSPs were observed in both titrations

(Figure 4-2). CSP values were plotted against residue number to demonstrate which residues are most likely involved in the interaction. The difference between the two CSP plots is minimal, thus the incorporation of Ub covalently bound to the catalytic cysteine of E2-25k has hardly any observable effect on the non-covalent interaction between Ub and E2-25k.

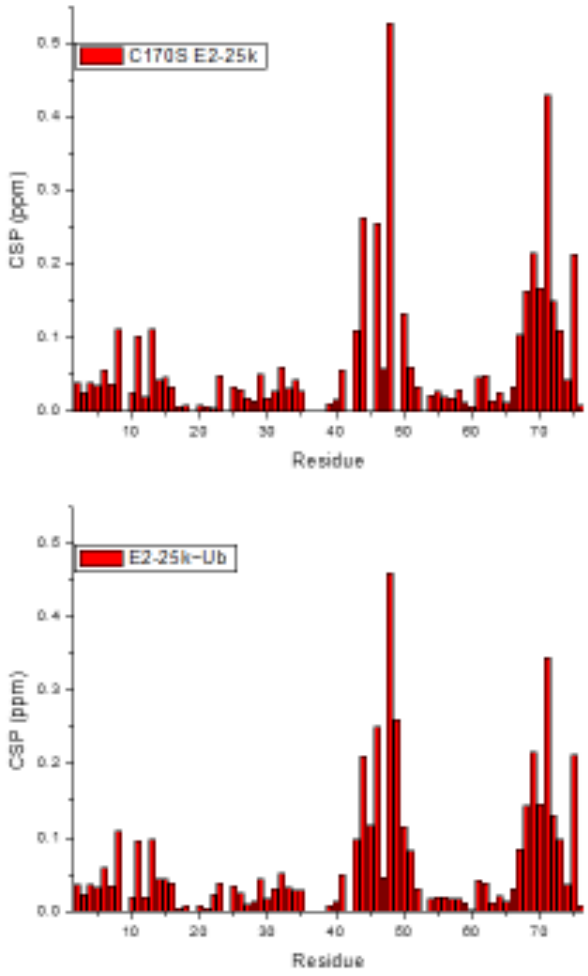

Figure 4-2: CSP plot of NMR titrations of ^{15}N Ub with E2-25k~Ub disulfide.

Top: E2-25k C170S with ^{15}N Ub. Bottom: E2-25k~Ub disulfide with ^{15}N Ub.

4.3.2 Titration of Ub into E2-25~Ub(^{15}N)

E2-25k~Ub disulfide with the Ub domain isotopically labeled (^{15}N) was created by incorporating ^{15}N G76C Ub into the disulfide reaction. With this construct, the non-covalent interactions that Ub may have with E2-25k when covalently attached to the catalytic cysteine can be observed. HSQC spectra of both ^{15}N G76C Ub and of E2-25k~(^{15}N)Ub were collected. A CSP plot comparing E2-25~Ub(^{15}N) to ^{15}N G76C Ub identifies the residues involved in the interface created between E2-25k and Ub while thioester linked. Residues which had corresponding CSP values greater than 0.05 were mapped on the surface of Ub (Figure 4-3).

E2-25k~Ub(^{15}N) was titrated with unlabeled Ub, but no significant CSPs were observed (data not shown). Results show that if there is a conformational change upon covalent modification of E2-25k by Ub, it cannot be observed on either ubiquitin domain. The possible interface between donor Ub and E2-25k has been characterized by the CSP plot and surface map.

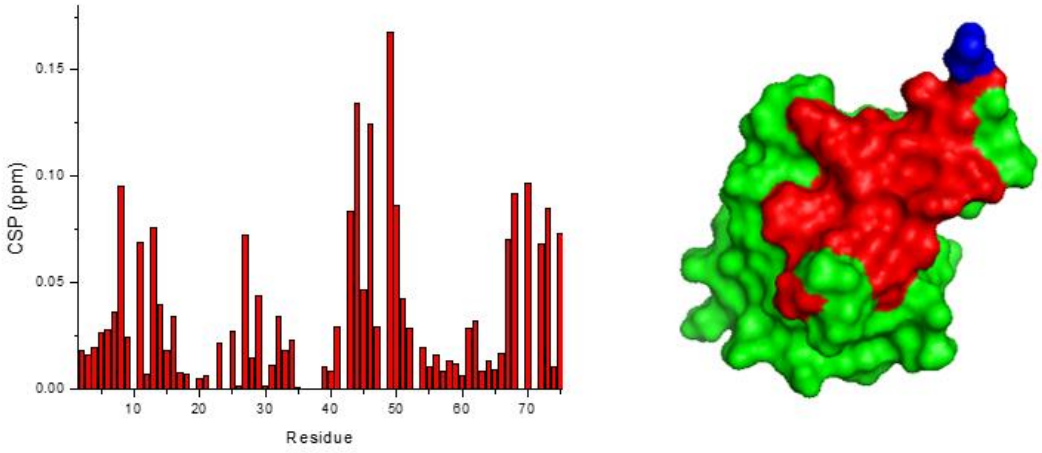

Figure 4-3: Chemical shift perturbations upon formation of E2-25k~Ub disulfide. CSP plot comparing G76C Ub to E2-25k~Ub; residues with CSP>0.05 mapped on surface of solution structure of Ub (pdb:1D3Z, red), C76 shown as blue.

Chapter 5: Study of Rub1/Ub chimera proteins

5.1 Introduction

There are seven major regions of dissimilarity between Rub1 and Ub ranging from three to eight amino acids in length (Figure 5-1). These regions will be referred to as I to VII, and the chimeras made with these mutations will be named accordingly. For example, Ub-I is ubiquitin in which its residues 2-4 are switched with that of Rub1 (QIF→IVK).

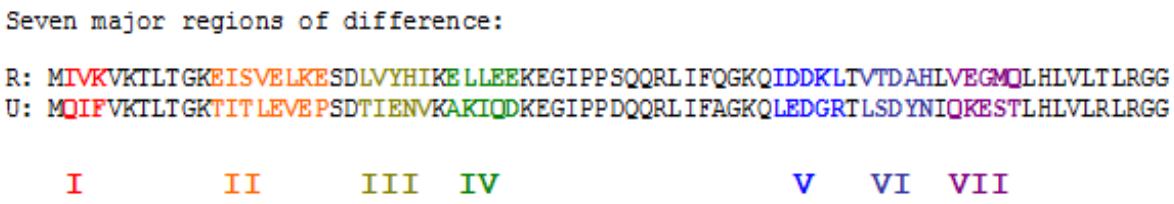

Figure 5-1: Regions of dissimilarity between the amino acid sequences of Rub1 (R) and Ub (U) grouped I to VII.

5.2 In vitro ubiquitination reactions with chimeric proteins

All seven of the Ub-Rub1 chimeras were expressed and purified as explained in the Materials and Methods section. These purified chimeras were tested for their ability to create polyubiquitin chains by a standard *in vitro* ubiquitination reaction. Similar to wild-type Ub, Ub-I through Ub-V chimeras retained their ability to form polyubiquitin chains. Conversely, Ub-VI and Ub-VII did not react as efficiently as

wild-type Ub (Figure 5-2). This indicates that the corresponding residues (56-60 and 62-66) are required for efficient Ub polymerization by E2-25k. This finding directed us to create Rub1 chimeras in which regions VI and VII are switched to that of Ub.

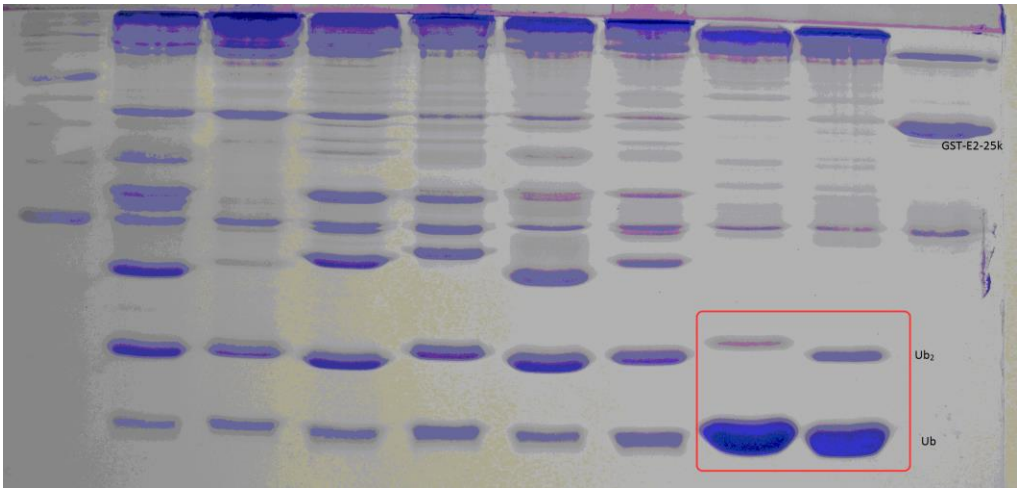

Figure 5-2: E2-25k catalyzed *in vitro* ubiquitination reactions using Ub/Rub1 chimeras. SDS-PAGE gel of ubiquitination reactions stained with Coomassie Brilliant Blue. Lane 1, protein marker; lane 2, WT-Ub; lanes 3-9, Ub-I to Ub-VII; lane 10, E1 and E2-25k. Boxed in red are Ub-VI and Ub-VII monomer and dimer.

5.2.1 Rub1/Ub chimeras

In accordance with previous studies, wild-type Rub1 does not form chains. Surprisingly, mutations in regions VI and/or VII allows for the formation of a novel Rub1-Rub1 dimer using the enzymatic machinery of ubiquitin (Figure 5-3). The efficiency of this reaction is very low, but the formation of these Rub1-Rub1 dimers reinforces the notion that residues 56-60 and 62-66 are important in the E2-25k mediated catalysis.

Although wild-type Rub1 does not react to form poly-Rub1 chains, it does covalently attach to E2-25k as evidenced by the bands that form above E2-25k on the gel. This demonstrates its ability to get activated by ubiquitin E1, undergo transthiolation onto E2-25k, and ultimately form isopeptide bonds with the lysine resides of E2-25k. The auto-rubylation of E2-25k is observed in all Rub1 mutants.

Despite the high similarity between Rub1 and ubiquitin, E2-25k is able to preferentially select ubiquitin for the catalysis of the formation of free K48-linked polyubiquitin chains. Since Rub1 can covalently attach to one or several lysine(s) of E2-25k in *in vitro* ubiquitination reactions, it can be assumed that the thioester intermediate Rub1~E2-25k is formed. It cannot undergo the next step, which would be the formation of Rub1 chains by the nucleophilic attack of the thioester by the lysine residue of an acceptor Rub1.

This activity may be prevented due to the unfavorable conformation that the acceptor Rub1 might take upon binding to E2-25k. Rub1 may use a different surface than ubiquitin in its non-covalent interaction with E2-25k, or it simply may not bind tightly enough for the reaction to occur. These factors can be tested using NMR titrations to monitor the binding of either Rub1 or ubiquitin to E2-25k at the atomic level.

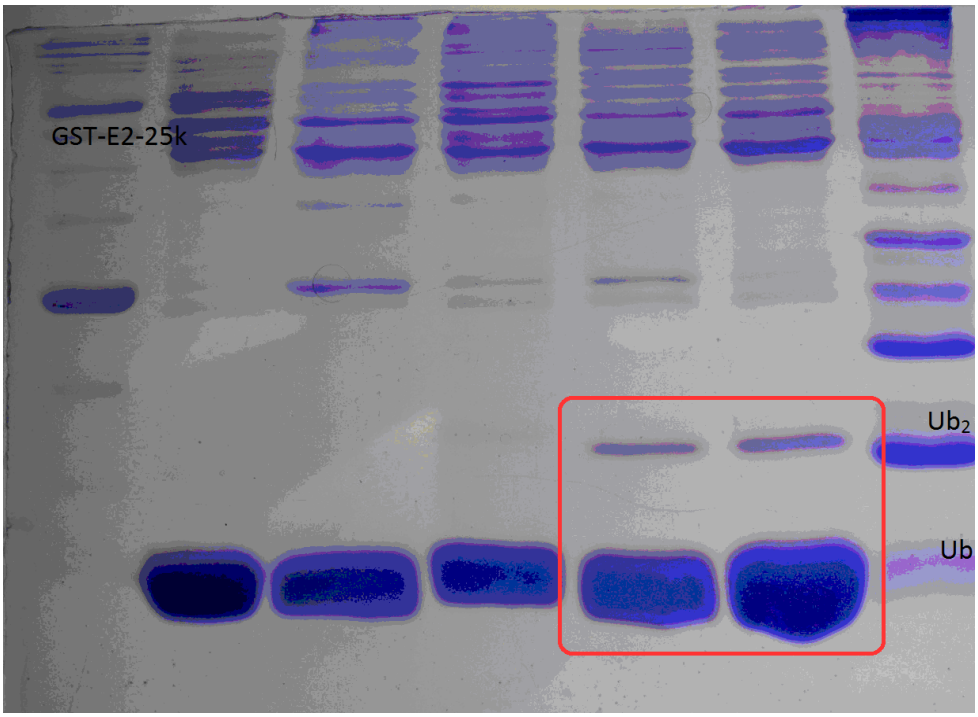

Figure 5-3: E2-25k catalyzed *in vitro* ubiquitination reactions using Rub1/Ub chimeras. SDS-PAGE gel of ubiquitination reactions stained with Coomassie Brilliant Blue. Lane 1, protein marker; lane 2, WT-Rub1; lane 3, Rub1-VI; lane 4, Rub1-VII, lane 5, Rub1-VI-E63K; lane 6, Rub1-VI-VII; lane 7, WT-Ub (control). Boxed in red are the novel mutant Rub1-Rub1 dimers.

5.3 NMR titrations with E2-25k

The difference between Rub1 and ubiquitin in their ability to form chains using the ubiquitin-conjugating enzyme E2-25k may lie in their respective non-covalent interactions. The interaction between Rub1 and E2-25k was assayed using an NMR titration experiment in which a series of ^{1}H-^{15}N HSQC spectra were collected at each titration point. Bacterially expressed Rub1 was grown in minimal media in which the sole nitrogen source was ^{15}N labeled NH_4Cl, ensuring the

incorporation of ^{15}N in the cellular synthesis of Rub1. After purification, an NMR sample of ^{15}N Rub1 was prepared at a concentration of 200 µM. The HSQC spectra of Rub1 resulted in a good distribution of peaks that were previously assigned.

Unlabeled E2-25k was added in increasing amounts and HSQC spectra were collected upon each addition of E2-25k. At a ratio of [Rub1]:[E2-25k] = 1:10 the peaks no longer shifted so it is assumed that the titration reached saturation. Residues with a CSP value greater than 0.07 were mapped on the surface of an NMR solution structure of Rub1[19] to highlight the surface of interaction. For comparison, the same titration experiment was performed on ^{15}N labeled ubiquitin and unlabeled E2-25k; the CSP plot and mapped surface are shown (Figure 5-4). The CSP values determined at each point in the titration for each residue were plotted and fit to a simple binding curve. Resulting from this analysis, the K_d of this interaction was estimated to be 310 ± 70 µM which is essentially equal to the K_d of the interaction between ubiquitin and E2-25k which is 400 ± 100 µM.

Both Rub1 and ubiquitin have similar interactions with E2-25k, which is demonstrated by their binding surfaces and near identical K_d values. Ubiquitin uses its canonical hydrophobic binding surface, residues L8, I44, and V70[21]; these residues are conserved between ubiquitin and Rub1, so the similarities in their interactions are not surprising. Based on the mutational studies described earlier, it seems that residues 56-60 and 62-66 are implicated in the catalysis of chain formation. Interestingly, these residues are not significantly perturbed upon titration of E2-25k in either Rub1 or ubiquitin, so it seems that they serve some unclear function that is secondary to binding. Possibly, these residues affect the positioning of the ε-amine

group of K48 which is very important for the mechanism by which the acceptor UBL attacks the thioester group formed at the active cysteine of E2-25k. If the positioning of K48 in Rub1 deviates from that of ubiquitin it may render it unfavorable to react, removing it from proximity to the thioester which would decrease the probability of a nucleophilic attack.

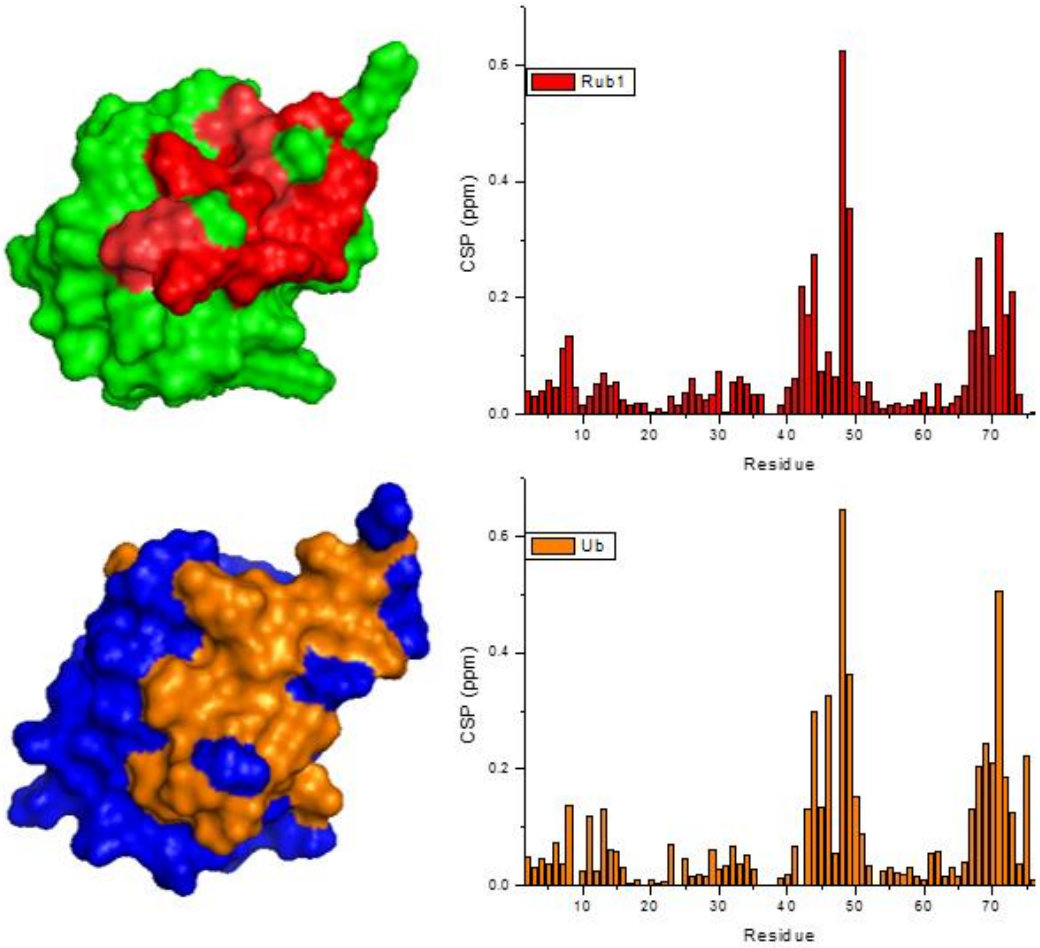

Figure 5-4: Saturation CSPs observed in titrations of 15N Rub1 and 15N Ub with unlabeled E2-25k. Solution structure of Rub1 (green) with significant CSPs (>0.07, red) mapped on the surface. Solution structure of Ub (blue, 1D3Z) with significant CSPs (>0.07, orange) mapped on the surface.

Chapter 6: Discussion

6.1 Cyclic K48-linked Ub_2

6.1.1 Summary

Cyclic K48-linked Ub_2 ($cycUb_2$) was formed and isolated from E2-25k catalyzed *in vitro* ubiquitination reactions as a result of a sequence of biochemical purification steps. The presence of $cycUb_2$ was validated by mass spectrometry; $cycUb_2$ is expected to have a mass of 18 Da less than that of acyclic Ub_2 due to the formation of a second isopeptide bond. Furthermore, NMR spectra of $cycUb_2$ show that the peak associated with the C-terminal residue, G76, has completely shifted to the conjugated position.

Ultimately a highly pure sample of $cycUb_2$ was used to form protein crystals for X-ray crystallography, from which a crystal structure was determined with good resolution (1.4 Å). By mapping the CSPs observed by NMR onto the crystal structure, it is apparent that the CSPs occur primarily at the hydrophobic interface between the two Ub domains. RDC and relaxation measurements are in good agreement with the crystal structure in terms of orientation and dynamics.

All attempts to characterize the structure and dynamics of $cycUb_2$ suggest that its structure is fixed in the closed conformation, which should hinder its ability to interact with ligands due to the sequestration of hydrophobic residues at the interface. To test this, $cycUb_2$ was titrated with

UQ1-UBA, UBA2, and UIM. From these titrations we find that cycUb$_2$ still binds these ligands despite its structural constraints. The CSPs observed upon binding are generally located at the hydrophobic interface, and upon titration in all cases, attenuation of specific residues was observed, which is usually indicative of tight binding. However, the K_d values determined for the interactions were all roughly 10-fold higher than that observed for K48-Ub$_2$ or monoUb. The stoichiometry of binding seems to be 1:2; one cycUb$_2$ per two UBA domains. HyTEMPO, a small paramagnetic molecule known to have an affinity for the hydrophobic patch of Ub, was added to cycUb$_2$ to see if it could access the hydrophobic residues of cycUb$_2$. Indeed, signal attenuations were observed in cycUb$_2$ upon incubation with HyTEMPO, with a similar pattern and intensity to what was observed for K48-Ub$_2$.

SANS data shows a discrepancy between solution data and crystal structure, indicating that there are some dynamics involved, which helps to explain how cycUb$_2$ is capable of interacting with ligands. DUB assays were performed and demonstrated the ability of OTUB1 to cleave cycUb$_2$. However, the rate of reaction was very slow, much slower than what was observed for K48-Ub$_2$. OTUB1 is able to recognize cycUb$_2$ well enough to bind it and cleave the isopeptide bonds, but not nearly as well as it does for K48-Ub$_2$. Nevertheless, this observation acts as an example for how the cell may deal with endogenous cyclic polyUb chains.

6.1.2 Future Direction

$CycUb_2$ is now characterized structurally and biochemically. We learned that $cycUb_2$ can bind ligands with lower affinities, which demonstrates its dynamic nature that allows for ligands to access the hydrophobic patch. Using a combination of CSP, RDC, relaxation, and SANS data, models can be created to explain such interactions.

The DUB activity observed for OTUB1 and the assumed interaction between OTUB1 and $cycUb_2$ is interesting and warrants further study. The mechanism by which OTUB1 recognizes the isopeptide of K48-linked chains is well studied. How does the current knowledge of OTUB1 mechanism apply to the cleavage of $cycUb_2$? The rate of reaction is considerably slower for cyclic chains when compared to acyclic. It may be interesting to quantitatively study the kinetics of the reaction to better understand the mechanism and interactions involved.

While there is published literature claiming the existence of $cycUb_2$ *in vivo*, the actual study itself is not entirely convincing. In my opinion, it is unclear if $cycUb_2$ is actually formed *in vivo* or is formed after cell lysis in the lysate which may contain E2-25k or potentially other E2/E3 systems capable of creating $cycUb_2$. In any case, my studies show that while it does have the ability to bind ligands, the binding affinities observed are weak enough to be considered physiologically irrelevant. Therefore, I do not believe there is enough evidence to merit any further investigation on $cycUb_2$ in the cell.

Chapter 7: Materials and Methods

7.1 Purification of proteins

7.1.1 Bacterial expression of recombinant proteins

The plasmid pET28 containing the gene for N-terminal (6x)His-tagged human E1 was transformed into *E. coli* BL21(DE3) *Rosetta* cells. Cells were grown at 37°C until OD_{600} = 0.6-0.8, then moved to 20°C before inducing with 1 mM IPTG, and continued growth at 20°C for 6h. Cells were centrifuged down and resuspended in 25 mL of lysis buffer (1X PBS pH 7.4, 2.5 μg/mL STI, 2.5 μg/mL leupeptin, 0.02% (v/v) Triton X-100) per 1L of cell culture, to which 0.4 mg/mL lysozyme, 10 μg/mL DNAse I, and 10 mM $MgCl_2$ were added. Lysate was purified through nickel affinity chromatography.

The plasmid pGEX containing the gene for GST-fused wild-type E2-25k was transformed into *E. coli* BL21(DE3) cells using autoinducing media at 37°C for 18h. The cells were centrifuged down and stored at -80°C before lysis. Cells were lysed in 25 mL of lysis buffer (1X PBS pH 7.4, 2.5 μg/mL STI, 2.5 μg/mL leupeptin, 0.02% (v/v) Triton X-100) per 1L of cell culture. Cleared lysate was purified through glutathione affinity chromatography from which GST-fused E2-25k was eluted. The same procedure was followed for UQ1-UBA and hHR23a-UBA2; both constructs used the same plasmid.

The plasmid pET28a containing the gene for N-terminal (6x)His-tagged USP5 (isoT) was transformed into *E. coli* BL21(DE3) cells using LB media supplemented with 150 mM glycerol. Cells were grown at 37°C until OD_{600} = 1.0, then moved to 18°C for an hour before adding 1 mM IPTG, and grown at 18°C for an additional 24-36h. Cells were centrifuged down and stored at -80°C before lysis. Cells were lysed in 25 mL of lysis buffer (1X PBS pH 7.4, 2.5 μg/mL STI, 2.5 μg/mL leupeptin, 0.02% (v/v) Triton X-100) per 1L of cell culture, to which 0.4 mg/mL lysozyme, 10 μg/mL DNAse I, and 10 mM $MgCl_2$ were added. Lysate was purified through nickel affinity chromatography.

The plasmid pET3a containing the gene for wild-type Ub was transformed into E. coli BL21(DE3) competent cells and expressed using autoinducing media at 37°C for 18h. The cells were centrifuged down and stored at -80°C before lysis. Cells were lysed in 25 mL of lysis buffer (1X PBS pH 7.4, 2.5 μg/mL STI, 2.5 μg/mL leupeptin, 0.02% (v/v) Triton X-100) per 1L of cell culture. Crude cell lysate was treated with perchloric acid added dropwise and centrifuged down to remove precipitated proteins. The resulting supernatant was dialyzed in 50 mM NH4Ac pH 4.5 before purifying via cation column chromatography.

The plasmid pTXB1 containing the gene for chitin-binding intein fusion proteins Ub or Rub1 was transformed into E. coli BL21(DE3) competent cells and expressed using autoinducing media at 37°C for 18h. The cells were centrifuged down and stored at -80°C before lysis. Cells were lysed

by sonication in 25 mL of lysis buffer (1X PBS pH 7.4, 2.5 μg/mL STI, 2.5 μg/mL leupeptin, 0.02% (v/v) Triton X-100) per 1L of cell culture. Cell lysate was loaded onto a column of chitin beads after which DTT was used to cleave Ub or Rub1 off the column. This procedure was followed for all Ub/Rub1 chimera proteins: WT Ub, Ub-I through Ub-VII, Ub-VII-E63K, WT Rub1, Rub1-VI, Rub1-VII, Rub1-VI-VII, Rub1-VI-E63K, and Rub1-E63K.

7.1.2 Purification of cycUb_2

K48-linked polyUb chains were formed via E2-25k mediated *in vitro* ubiquitination reactions. A mixture containing 500 nM E1, 20 μM E2-25k, and 500 μM Ub was incubated at 30°C for 16h in a buffer composed of 50 mM Tris pH 8.0, 2 mM ATP, 3 mM TCEP, 1X PBDM8. The ubiquitination reaction mixture was passed through a size exclusion column in 50 mM Tris pH 8.0, 130 mM NaCl, 0.02% NaN_3. Fractions containing Ub_2 were concentrated and buffer exchanged into 50 mM Tris pH 8.0, 25 mM NaCl. Ub_2 fractions were incubated in the presence of 200 nM isoT at 37°C for 6h. After incubation, acetic acid was added to a final concentration of 2% by volume, and the reaction mixture was dialyzed against 50 mM NH_4Ac pH 4.5. The resultant mixture, which should contain a mixture of cycUb_2 and monoUb, was passed through a cation exchange column. Gradient: 0-35% B, volume: 140 mL, 4 mL fractions.

7.2 NMR experiments

NMR experiments were performed at 296K on either a 600 MHz or 800 MHz spectrometer. NMR samples were usually prepared in 20 mM $NaPO_4$ pH 6.8 and 5% D_2O. For the titrations, a series of ^{1}H-^{15}N HMQC spectra were collected during titration of the ^{15}N labeled protein with the unlabeled ligand. CSPs were calculated using the equation $\Delta\delta = [(\Delta\delta_H)^2+(\Delta\delta_{N}/5)^2]^{1/2}$ where $\Delta\delta_H$ and $\Delta\delta_N$ are the changes in chemical shifts for ^{1}H and ^{15}N respectively.

7.3 Crystallization

Highly pure samples $cycUb_2$ and $cycUb_3$ were subject to screening using commercially available crystal screening solutions and a robotic protein crystallography dispenser. A solution containing 3.4 mg/mL $cycUb_2$ in 20 mM HEPES pH 7.4 buffer was screened using Qiagen NeXtal PEGs Suite. The best crystals formed in the following buffer condition: 0.2M $(NH_4)_3PO_4$, 20% (w/v) PEG 3350. Crystals were taken using 20% glycerol cryoprotectant and 80% mother liquor.

7.4 Mass spectrometry

Mass spectra were obtained using electrospray ionization (positive) with flow injection on JEOL AccuTOF-CS mass spectrometer, and analyzed using MagTran software.

7.5 SANS

SANS data was collected and analyzed by Dr. Carlos Castañeda in collaboration with Dr. Susan Krueger at NIST.

Appendix

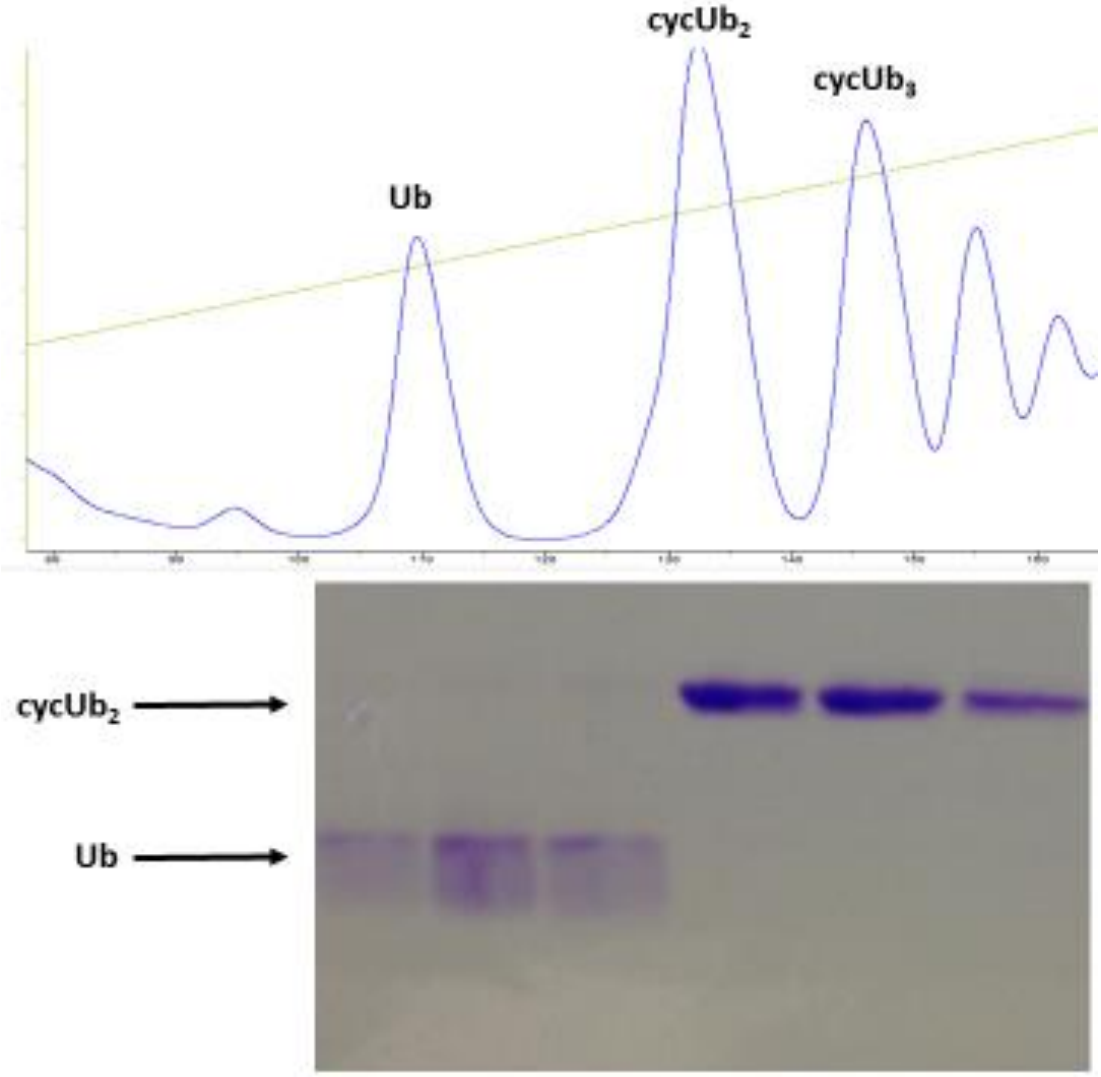

Figure A-1: Purification of cycUb$_2$ by cation exchange chromatography. A mixture containing monoUb and cyclic K48-linked polyUb chains of varying lengths was dialyzed into buffer containing 50 mM NH_4Ac pH 4.5 and subsequently passed through a HiTrap SP HP column. The chromatogram (top) demonstrates separation between monoUb, cycUb$_2$, and cycUb$_3$. Fractions were analyzed by SDS-PAGE (bottom).

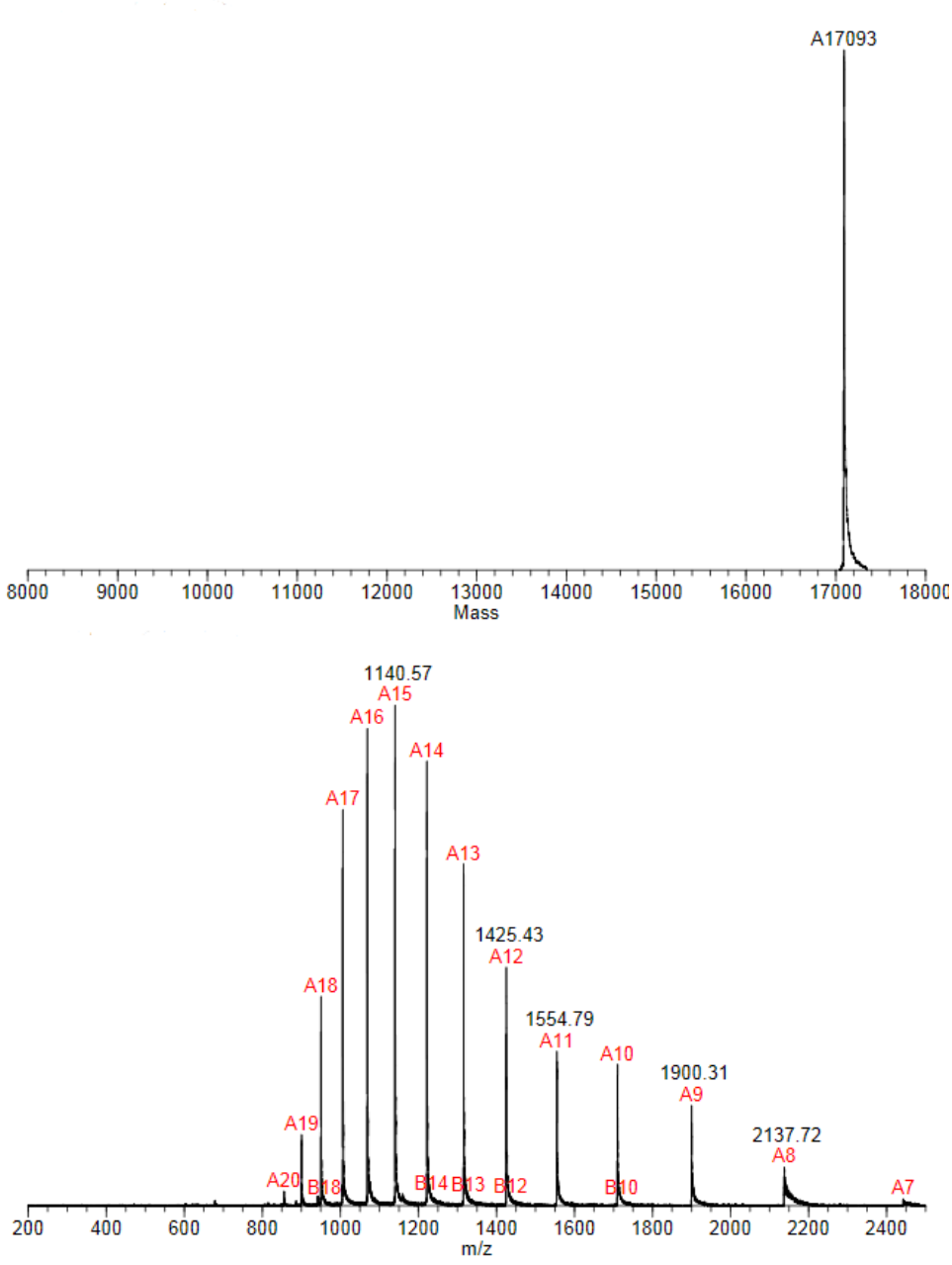

Figure A-2: ESI-MS spectrum of cycUb$_2$. The expected mass of cycUb$_2$ is 17094 Da; 17093 Da is observed.

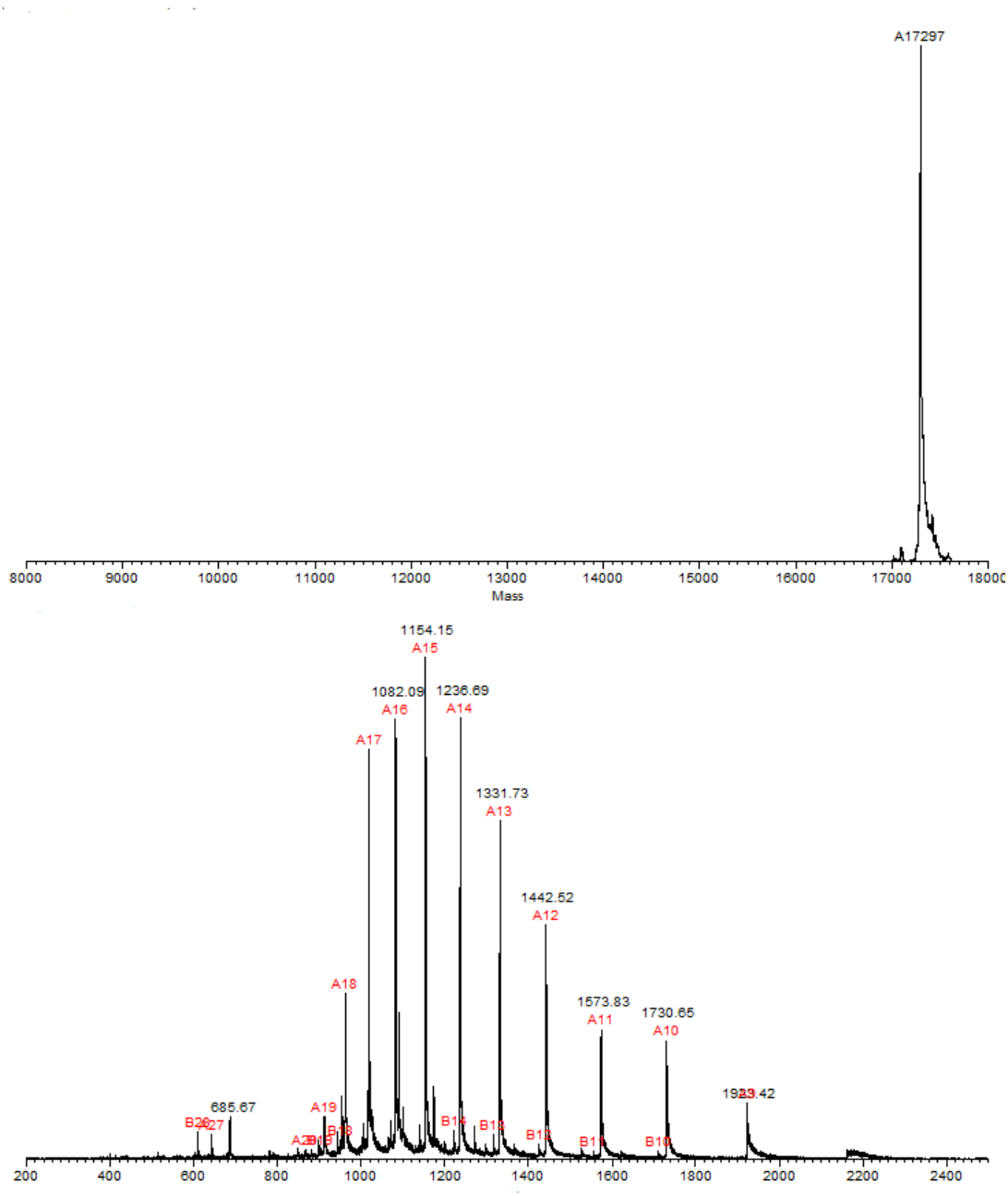

Figure A-3: ESI-MS spectrum of ^{15}N cycUb$_2$. The expected mass of ^{15}N cycUb$_2$ is 17294 Da; 17297 Da is observed.

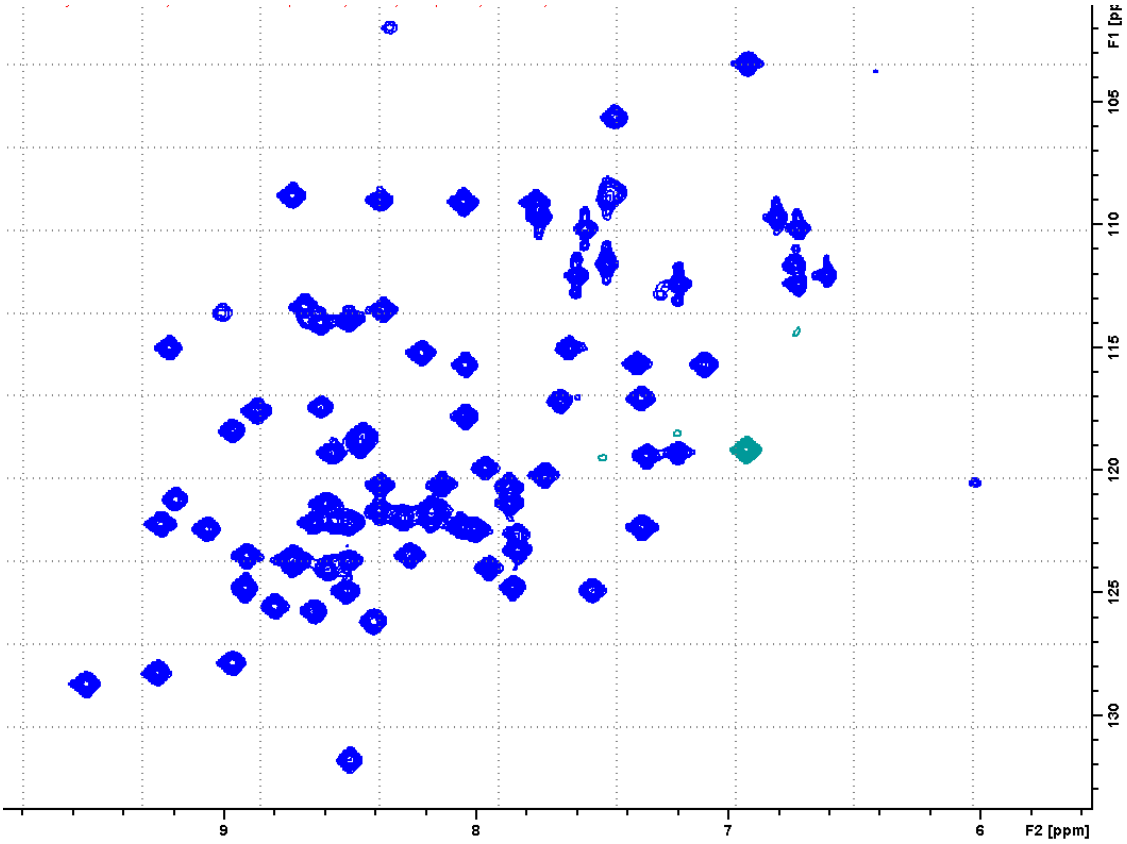

Figure A-4: 1H-15N HMQC (SOFAST) spectrum of cycUb$_2$. A solution of 200 µM ^{15}N cycUb$_2$ in 20 mM sodium phosphate buffer pH 6.8.

Residue	15N (ppm)	1H (ppm)	Residue	15N (ppm)	1H (ppm)	Residue	15N (ppm)	1H (ppm)
Q2	123.493	8.913	K27	118.818	8.461	D52	120.573	8.14
I3	115.239	8.22	A28	123.261	7.838	R54	119.447	7.329
F4	118.644	8.455	K29	120.202	7.733	T55	108.824	8.732
V5	122.212	9.254	I30	121.662	8.179	L56	117.82	8.046
K6	127.864	8.97	Q31	123.682	8.512	S57	113.464	8.373
T7	113.357	8.684	D32	119.92	7.969	D58	124.81	7.859
L8	121.194	9.195	K33	115.65	7.366	Y59	115.711	7.099
T9	105.623	7.455	E34	114.004	8.619	N60	115.713	8.046
G10	109.092	7.769	G35	108.982	8.384	I61	119.285	7.204
K11	122.346	7.346	I36	120.537	6.025	Q62	124.909	7.543
T12	121.385	8.602	D39	113.87	8.51	K63	120.627	8.384
I13	128.727	9.55	Q40	117.208	7.669	E64	115.02	9.221
T14	122.147	8.645	Q41	117.082	7.35	S65	115.053	7.637
L15	124.938	8.518	R42	122.16	8.507	T66	117.455	8.618
E16	122.459	8.007	L43	123.69	8.73	L67	128.284	9.267
V17	117.59	8.872	I44	122.413	9.069	H68	118.403	8.969
E18	119.298	8.575	F45	125.572	8.801	L69	123.487	8.264
S20	103.44	6.929	A46	131.838	8.503	V70	124.82	8.921
D21	124.003	7.954	G47	101.981	8.344	L71	122.7	7.841
T22	109.092	7.769	K48	120.702	7.871	R72	124.064	8.592
I23	121.677	8.387	Q49	122.052	8.565	L73	126.183	8.41
N25	121.363	7.87	L50	125.782	8.645	G75	113.625	9.009
V26	122.308	8.066	E51	121.968	8.292	G76	109.08	8.054

Table A-1: Assignment of chemical shifts observed for cycUb$_2$. ^{1}H-^{15}N HSQC spectrum of cycUb$_2$ obtained using Bruker 600 MHz NMR spectrometer in 20 mM $NaPO_4$ pH 6.8 buffer at 296K.

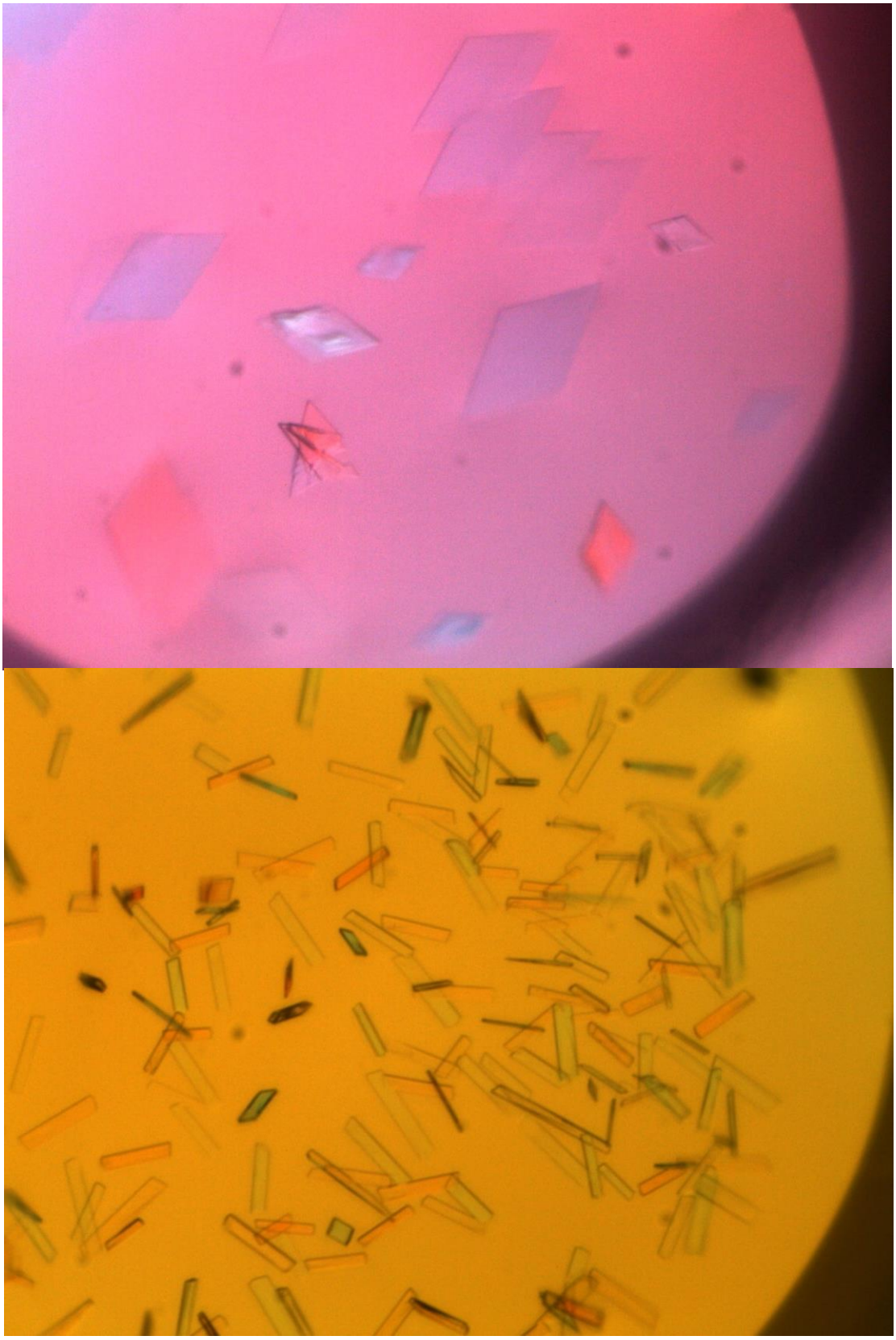

Figure A-5: Pictures of cycUb$_2$ crystals.

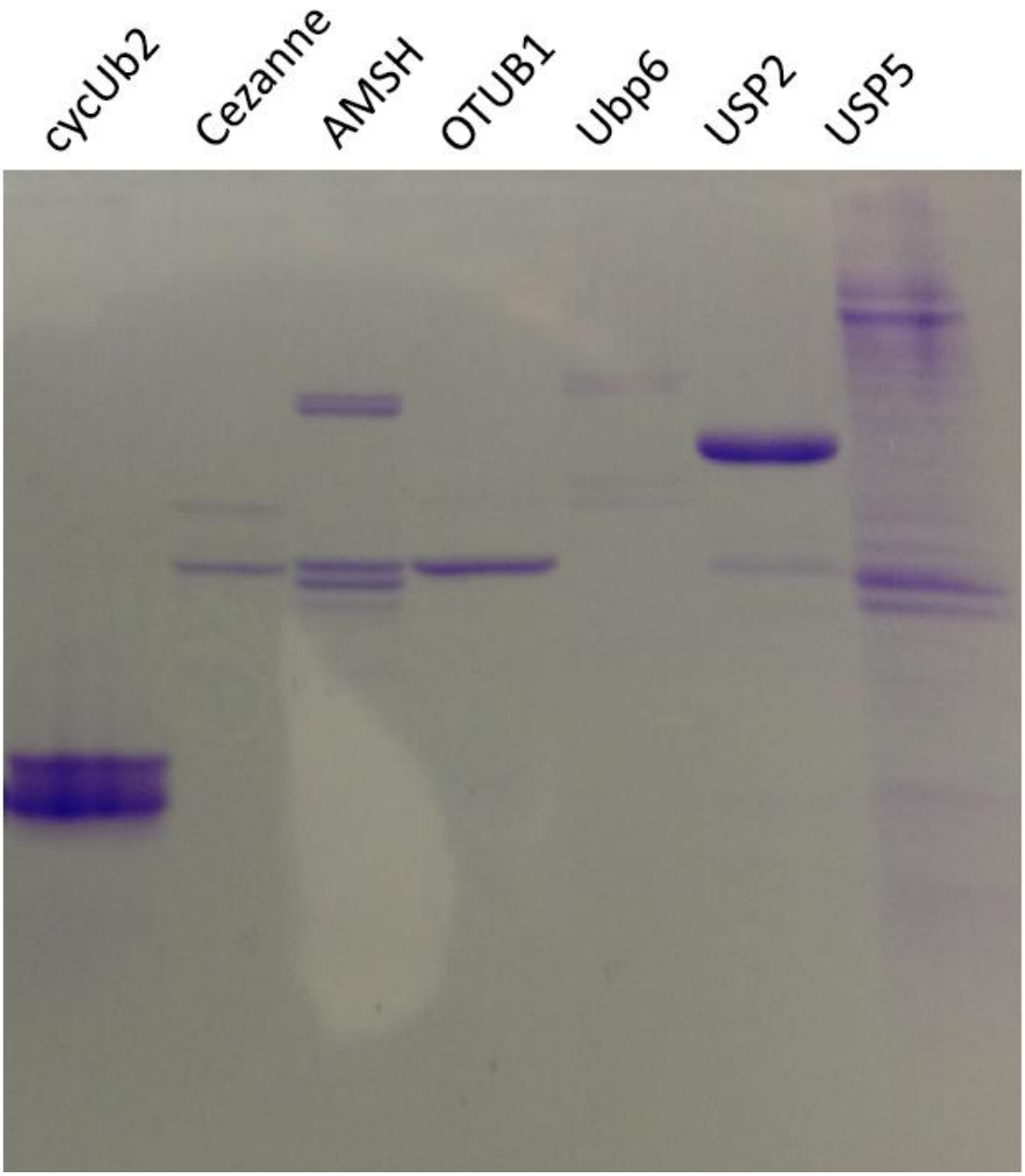

Figure A-6: Purified proteins used for DUB assay of cycUb$_2$. Proteins loaded on SDS-PAGE gel at same concentrations ([cycUb$_2$] = 20 μM, [DUB] = 2 μM) used in DUB reactions.

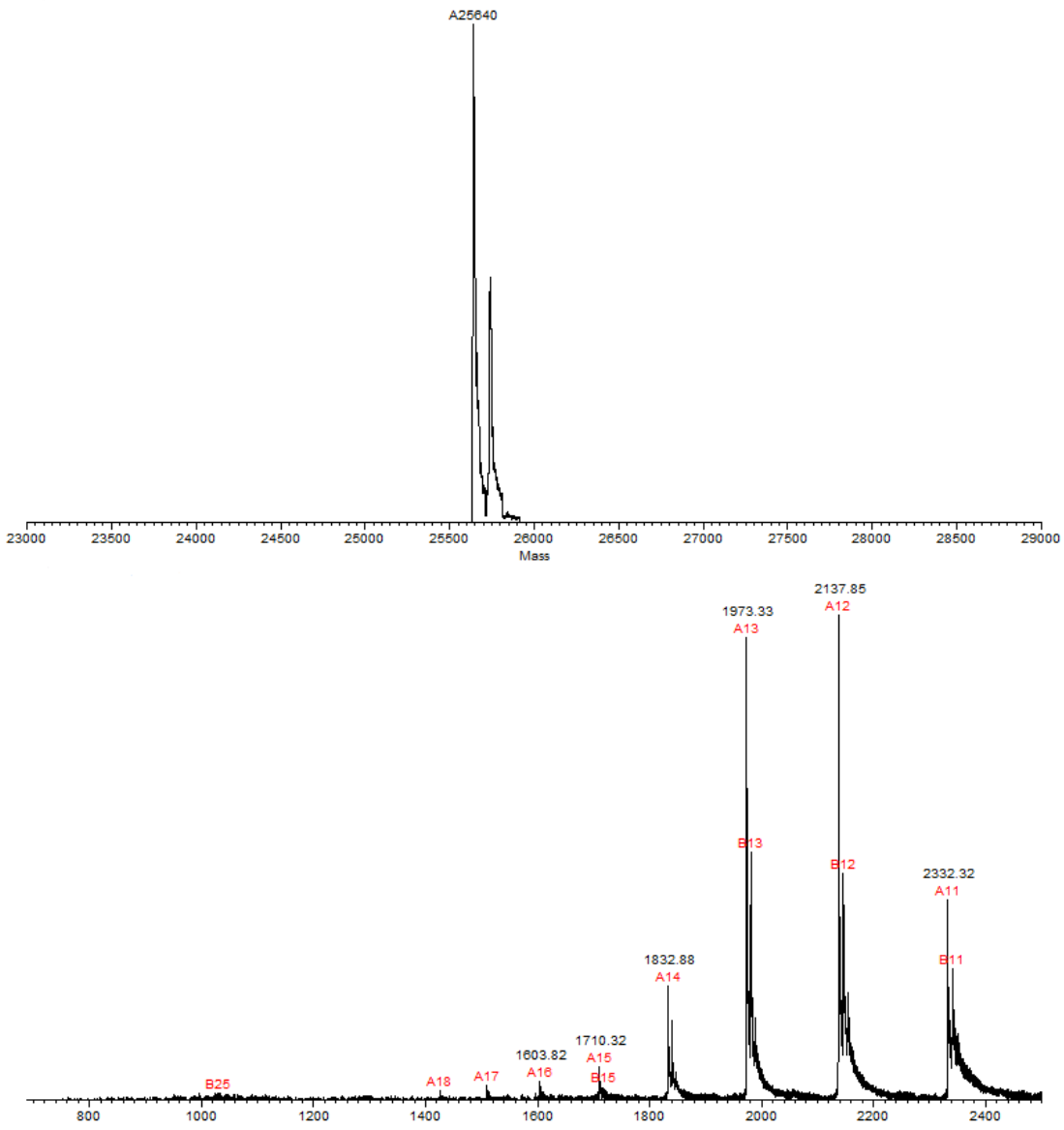

Figure A-7: ESI-MS spectrum of cycUb$_3$. The expected mass of cycUb$_3$ is 25640 Da; 25640 Da is observed.

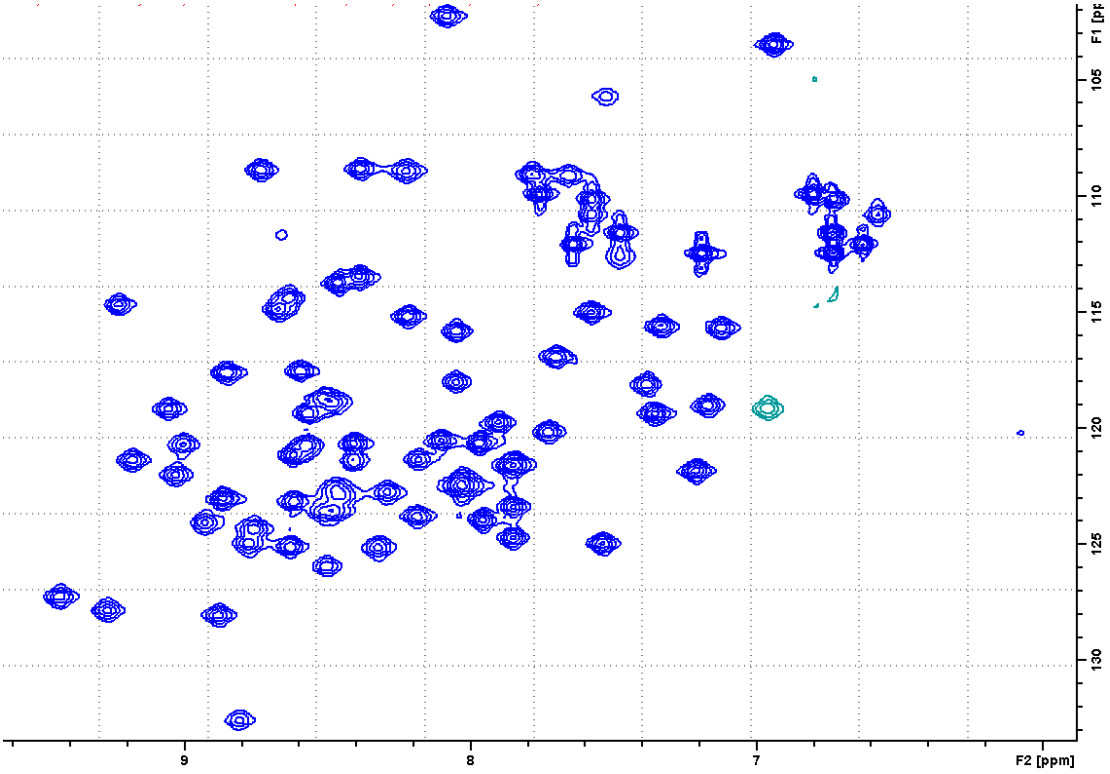

Figure A-8: 1H-15N HMQC (SOFAST) spectrum of cycUb$_3$. A solution of 200 µM ^{15}N cycUb$_3$ in 20 mM sodium phosphate buffer pH 6.8.

Residue	15N (ppm)	1H (ppm)	Residue2	15N (ppm)2	1H (ppm)2	Residue3	15N (ppm)3	1H (ppm)3
Q2	123.037	8.868	K27	118.838	8.494	E51	122.755	8.294
I3	115.214	8.223	A28	123.399	7.853	D52	120.544	8.106
F4	118.76	8.511	K29	120.177	7.73	R54	119.401	7.357
V5	121.387	9.186	I30	121.364	8.185	T55	108.905	8.737
K6	128.074	8.885	Q31	123.577	8.489	L56	118.022	8.054
T7	114.881	8.675	D32	119.749	7.906	S57	113.49	8.393
L8	120.725	9.008	K33	115.607	7.338	D58	124.736	7.854
T9	105.736	7.529	E34	114.393	8.639	Y59	115.703	7.127
G10	109.142	7.659	G35	108.841	8.388	N60	115.818	8.053
K11	121.852	7.215	I36	120.221	6.079	I61	119.033	7.173
T12	120.744	8.575	D39	113.754	8.467	Q62	124.976	7.542
I13	127.263	9.44	Q40	116.948	7.705	K63	120.675	8.41
T14	121.172	8.622	Q41	118.122	7.388	E64	114.679	9.234
L15	125.128	8.634	R42	122.889	8.461	S65	115.023	7.581
E16	122.49	8.032	L43	124.338	8.76	T66	117.546	8.597
V17	117.619	8.856	I44	122.021	9.033	L67	127.858	9.273
E18	119.377	8.57	F45	124.962	8.78	H68	119.17	9.059
S20	103.499	6.944	A46	132.589	8.812	L69	123.828	8.189
D21	123.973	7.961	G47	102.282	8.087	V70	124.065	8.931
T22	109.075	7.787	K48	120.649	7.972	L73	125.158	8.325
I23	121.415	8.412	Q49	123.181	8.62	G75	111.723	8.664
N25	121.601	7.854	L50	125.97	8.505	G76	108.94	8.228
V26	122.49	8.032						

Table A-2: Assignment of chemical shifts observed for cycUb$_3$. ^{1}H-^{15}N HSQC spectrum of cycUb$_3$ obtained using Bruker 600 MHz NMR spectrometer in 20 mM $NaPO_4$ pH 6.8 buffer at 296K.

Bibliography

1. Hershko, A.; Ciechanover, A., The ubiquitin system. *Annu Rev Biochem* **1998,** *67*, 425-79.
2. Pickart, C. M., Mechanisms underlying ubiquitination. *Annu Rev Biochem* **2001,** *70*, 503-33.
3. Chau, V.; Tobias, J. W.; Bachmair, A.; Marriott, D.; Ecker, D. J.; Gonda, D. K.; Varshavsky, A., A multiubiquitin chain is confined to specific lysine in a targeted short-lived protein. *Science* **1989,** *243* (4898), 1576-83.
4. Pickart, C. M.; Fushman, D., Polyubiquitin chains: polymeric protein signals. *Curr Opin Chem Biol* **2004,** *8* (6), 610-6.
5. Wilkinson, K. D.; Audhya, T. K., Stimulation of ATP-dependent proteolysis requires ubiquitin with the COOH-terminal sequence Arg-Gly-Gly. *J Biol Chem* **1981,** *256* (17), 9235-41.
6. Capili, A. D.; Lima, C. D., Taking it step by step: mechanistic insights from structural studies of ubiquitin/ubiquitin-like protein modification pathways. *Curr Opin Struct Biol* **2007,** *17* (6), 726-35.
7. Ye, Y.; Rape, M., Building ubiquitin chains: E2 enzymes at work. *Nat Rev Mol Cell Biol* **2009,** *10* (11), 755-64.
8. Olsen, S. K.; Capili, A. D.; Lu, X.; Tan, D. S.; Lima, C. D., Active site remodelling accompanies thioester bond formation in the SUMO E1. In *Nature*, England, 2010; Vol. 463, pp 906-12.

9. Jin, J.; Li, X.; Gygi, S. P.; Harper, J. W., Dual E1 activation systems for ubiquitin differentially regulate E2 enzyme charging. *Nature* **2007,** *447* (7148), 1135-8.

10. van Wijk, S. J.; Timmers, H. T., The family of ubiquitin-conjugating enzymes (E2s): deciding between life and death of proteins. In *FASEB J*, United States, 2010; Vol. 24, pp 981-93.

11. Kim, H. C.; Huibregtse, J. M., Polyubiquitination by HECT E3s and the determinants of chain type specificity. *Mol Cell Biol* **2009,** *29* (12), 3307-18.

12. Deshaies, R. J.; Joazeiro, C. A., RING domain E3 ubiquitin ligases. *Annu Rev Biochem* **2009,** *78*, 399-434.

13. Wenzel, D. M.; Stoll, K. E.; Klevit, R. E., E2s: structurally economical and functionally replete. *Biochem J* **2011,** *433* (1), 31-42.

14. Chen, Z. J.; Niles, E. G.; Pickart, C. M., Isolation of a cDNA encoding a mammalian multiubiquitinating enzyme (E225K) and overexpression of the functional enzyme in Escherichia coli. *J Biol Chem* **1991,** *266* (24), 15698-704.

15. Haldeman, M. T.; Xia, G.; Kasperek, E. M.; Pickart, C. M., Structure and function of ubiquitin conjugating enzyme E2-25K: the tail is a core-dependent activity element. *Biochemistry* **1997,** *36* (34), 10526-37.

16. Wilson, R. C.; Edmondson, S. P.; Flatt, J. W.; Helms, K.; Twigg, P. D., The E2-25K ubiquitin-associated (UBA) domain aids in polyubiquitin chain synthesis and linkage specificity. *Biochem Biophys Res Commun* **2011,** *405* (4), 662-6.

17. van der Veen, A. G.; Ploegh, H. L., Ubiquitin-like proteins. *Annu Rev Biochem* **2012,** *81*, 323-57.

18. Whitby, F. G.; Xia, G.; Pickart, C. M.; Hill, C. P., Crystal structure of the human ubiquitin-like protein NEDD8 and interactions with ubiquitin pathway enzymes. *J Biol Chem* **1998,** *273* (52), 34983-91.

19. Singh, R. K.; Zerath, S.; Kleifeld, O.; Scheffner, M.; Glickman, M. H.; Fushman, D., Recognition and cleavage of related to ubiquitin 1 (Rub1) and Rub1-ubiquitin chains by components of the ubiquitin-proteasome system. *Mol Cell Proteomics* **2012,** *11* (12), 1595-611.

20. Ryabov, Y.; Fushman, D., Interdomain mobility in di-ubiquitin revealed by NMR. *Proteins* **2006,** *63* (4), 787-96.

21. Varadan, R.; Walker, O.; Pickart, C.; Fushman, D., Structural properties of polyubiquitin chains in solution. *J Mol Biol* **2002,** *324* (4), 637-47.

22. Cook, W. J.; Jeffrey, L. C.; Carson, M.; Chen, Z.; Pickart, C. M., Structure of a diubiquitin conjugate and a model for interaction with ubiquitin conjugating enzyme (E2). *J Biol Chem* **1992,** *267* (23), 16467-71.

23. Beal, R.; Deveraux, Q.; Xia, G.; Rechsteiner, M.; Pickart, C., Surface hydrophobic residues of multiubiquitin chains essential for proteolytic targeting. *Proc Natl Acad Sci U S A* **1996,** *93* (2), 861-6.

24. Zhang, D.; Raasi, S.; Fushman, D., Affinity makes the difference: nonselective interaction of the UBA domain of Ubiquilin-1 with monomeric ubiquitin and polyubiquitin chains. *J Mol Biol* **2008,** *377* (1), 162-80.

25. Varadan, R.; Assfalg, M.; Raasi, S.; Pickart, C.; Fushman, D., Structural determinants for selective recognition of a Lys48-linked polyubiquitin chain by a UBA domain. *Mol Cell* **2005,** *18* (6), 687-98.

26. Yao, T.; Cohen, R. E., Cyclization of polyubiquitin by the E2-25K ubiquitin conjugating enzyme. *J Biol Chem* **2000,** *275* (47), 36862-8.

27. Sokratous, K.; Strachan, J.; Roach, L. V.; Layfield, R.; Oldham, N. J., Cyclisation of Lys48-linked diubiquitin in vitro and in vivo. *FEBS Lett* **2012,** *586* (23), 4144-7.

28. Sokratous, K.; Roach, L. V.; Channing, D.; Strachan, J.; Long, J.; Searle, M. S.; Layfield, R.; Oldham, N. J., Probing affinity and ubiquitin linkage selectivity of ubiquitin-binding domains using mass spectrometry. *J Am Chem Soc* **2012,** *134* (14), 6416-24.

29. Hirano, T.; Serve, O.; Yagi-Utsumi, M.; Takemoto, E.; Hiromoto, T.; Satoh, T.; Mizushima, T.; Kato, K., Conformational dynamics of wild-type Lys-48-linked diubiquitin in solution. *J Biol Chem* **2011,** *286* (43), 37496-502.

30. Ye, Y.; Blaser, G.; Horrocks, M. H.; Ruedas-Rama, M. J.; Ibrahim, S.; Zhukov, A. A.; Orte, A.; Klenerman, D.; Jackson, S. E.; Komander, D., Ubiquitin chain conformation regulates recognition and activity of interacting proteins. *Nature* **2012,** *492* (7428), 266-70.